First Search for Heavy Neutral Leptons with IceCube DeepCore

Dissertation
zur Erlangung des akademischen Grades
doctor rerum naturalium
(Dr. rer. nat.)

im Fach: Physik
Spezialisierung: Experimentalphysik

eingereicht an der
Mathematisch-Naturwissenschaftlichen Fakultät
der Humboldt-Universität zu Berlin

von
Leander Fischer M. Sc.
geboren am 24. Oktober 1992
in Heidelberg

Präsidentin der Humboldt-Universität zu Berlin
Prof. Dr. Julia von Blumenthal

Dekanin der Mathematisch-Naturwissenschaftlichen Fakultät
Prof. Dr. Caren Tischendorf

Zusammenfassung

Zusammenfassung . . .

Abstract

Abstract . . .

Todo list

Contents

List of Figures

List of Tables

Standard Model Neutrinos and Beyond

1

1.1 The Standard Model

The *Standard Model (SM)* of particle physics is a Yang-Mills theory [1] providing very accurate predictions of weak, strong, and *electromagnetic (EM)* interactions. It is a relativistic quantum field theory that relies on gauge invariance, where all matter is made up of fermions, which are divided into quarks and leptons, and bosons describe the interactions between the fermions that have to fulfil the overall symmetry of the theory. Leptons are excitations of Dirac-type fermion fields.

The initial idea of the theory is associated with the works of Weinberg [2], Glashow [3], and Salam [4], that proposed a unified description of EM and weak interactions as a theory of a spontaneously broken SU(2) x U(1) symmetry for leptons, predicting a neutral massive vector boson Z^0, a massive charged vector boson $W^\pm$, and a massless photon γ as the gauge bosons. The Higgs mechanism [5], describing the breaking of the symmetry, predicts the existence of an additional scalar particle, the Higgs boson, giving the $W^\pm$ and Z^0 bosons their mass. The Higgs boson was discovered in 2012 at the LHC [6, 7].

Gell-Mann and Zweig proposed the quark model in 1964 [8, 9], which was completed by the discovery of non-abelian gauge theories [10] to form the SU(3) symmetry of the strong interaction called *quantum chromodynamics (QCD)*. QDC describes the interaction between quarks and gluons which completed the full picture of the SM in the mid-1970s. Together with the electroweak theory, the SM is a $SU(3)_C$ x $SU(2)_L$ x $U(1)_Y$ local gauge symmetry, with the conserved quantities C, *color*, L, *left-handed chirality*, and Y, *weak hypercharge*

In the following, the basic properties of the SM are described, following the derivations of [11, 12].

1.1.1 Fundamental Fields

Fermions in the SM are Weyl fields with either *left-handed (LH)* or *right-handed (RH)* chirality, meaning they are eigenvectors of the chirality operator γ_5 with $\gamma_5 \psi_{R/L} = \pm \psi_{R/L}$. Only LH particles transform under $SU(2)_L$. The Higgs field is a complex scalar field, a doublet of $SU(2)_L$, which is responsible for the spontaneous symmetry breaking of $SU(2)_L$ x $U(1)_Y$ to $U(1)_{EM}$. Local gauge transformations of the fields are given by

$$\psi \to e^{ig\theta^a(x)T^a} \psi \,, \tag{1.1}$$

where g is the coupling constant, $\theta^a(x)$ are the parameters of the transformation, and T^a are the generators of the group, with a counting them. The number of bosons is dependent on the generators of the symmetry groups, while the strength is defined by the coupling constants. There are eight massless gluons corresponding to the generators of the $SU(3)_C$ group. These

[1]: Yang et al. (1954), "Conservation of Isotopic Spin and Isotopic Gauge Invariance"

[2]: Weinberg (1967), "A Model of Leptons"

[3]: Glashow (1961), "Partial-symmetries of weak interactions"

[5]: Higgs (1964), "Broken symmetries, massless particles and gauge fields"

[6]: Chatrchyan et al. (2012), "Observation of a New Boson at a Mass of 125 GeV with the CMS Experiment at the LHC"

[7]: Aad et al. (2012), "Observation of a new particle in the search for the Standard Model Higgs boson with the ATLAS detector at the LHC"

[8]: Gell-Mann (1964), "A Schematic Model of Baryons and Mesons"

[9]: Zweig (1964), "An SU(3) model for strong interaction symmetry and its breaking. Version 2"

[11]: Giunti et al. (2007), *Fundamentals of Neutrino Physics and Astrophysics*

[12]: Schwartz (2013), *Quantum Field Theory and the Standard Model*

mediate the strong force which conserves color charge. The $W_1, W_2, W_3,$ and B boson fields of the SU(2)$_L$ x U(1)$_Y$ group are mixed into the massive bosons through spontaneous symmetry breaking as

$$W^\pm = \frac{1}{\sqrt{2}}(W_1 \mp iW_2) \qquad (1.2)$$

and

$$Z^0 = \cos\theta_W W_3 - \sin\theta_W B , \qquad (1.3)$$

with θ_W being the *Weinberg angle*. The massless photon field is given by

$$A = \sin\theta_W W_3 + \cos\theta_W B \qquad (1.4)$$

and its conserved quantity is the EM charge Q, which depends on the weak hypercharge, Y, and the third component of the weak isospin, T_3, as $Q = T_3 + Y/2$.

	Type			Q
quarks	u	c	t	+2/3
	d	s	b	-1/3
leptons	ν_e	ν_μ	ν_τ	0
	e	μ	τ	-1

Table 1.1: Fermions in the Standard Model. Shown are all three generations of quarks and leptons with their electric charge Q.

Fermions are divided into six quarks and six leptons. Weak, strong, and EM force act on the quarks, and they are always found in bound form as baryons or mesons. Leptons do not participate in the strong interaction and only the electrically charged leptons are massive and are effected by the EM force, while neutrinos are massless and only interact via the weak force. Each charged lepton has an associated neutrino, which it interacts with in *charged-current (CC)* weak interactions, that will be explained in more detail in Section 1.1.4. The fermions are listed in Table 1.1.

1.1.2 Electroweak Symmetry Breaking

To elaborate the process of spontaneous symmetry breaking through which the gauge bosons of the weak interaction acquire their masses, the Lagrangian of the Higgs field is considered as

$$\mathscr{L}_{\text{Higgs}} = (D_\mu \Phi^\dagger)(D^\mu \Phi) - \lambda\left(\Phi^\dagger\Phi - \frac{v^2}{2}\right)^2 , \qquad (1.5)$$

with parameters λ and v, where λ is assumed to be positive. Φ is the Higgs doublet, which is defined as

$$\Phi = \begin{pmatrix} \Phi^+ \\ \Phi^0 \end{pmatrix} , \qquad (1.6)$$

with the charged component Φ^+ and the neutral component Φ^0. The covariant derivative is given by

$$D_\mu = \partial_\mu - ig_2\frac{\sigma^i}{2}W_\mu^i - \frac{1}{2}ig_1 B_\mu , \qquad (1.7)$$

with the Pauli matrices σ^i and the gauge boson fields W_μ^i and B_μ of the SU(2)$_L$ and U(1)$_Y$ groups, respectively. The coupling constants g_2 and g_1 are the respective coupling constants which are related to the Weinberg angle as $\tan\theta_W = \frac{g_1}{g_2}$. The Higgs potential has a non-zero *vacuum expectation value (vev)* at the minimum of the potential at $\Phi^\dagger\Phi = \frac{v^2}{2}$. Since the vacuum is electrically neutral, it can only come from a neutral component of the Higgs

doublet as

$$\Phi_{\text{vev}} = \frac{1}{\sqrt{2}} \begin{pmatrix} 0 \\ v \end{pmatrix}. \tag{1.8}$$

1.1.3 Fermion Masses

The mass term for charged fermions with spin-1/2 is given by

$$\mathcal{L}_{\text{Dirac}} = m(\bar{\Psi}_R \Psi_L - \bar{\Psi}_L \Psi_R), \tag{1.9}$$

composed of the product of LH and RH Weyl spinors $\Psi_{L/R}$. This term is not invariant under SU(2)$_L$ x U(1)$_Y$ gauge transformations, but adding a Yukawa term

$$\mathcal{L}_{\text{Yukawa}} = -Y^e \bar{L}_L \Phi e_R + h.c., \tag{1.10}$$

coupling the fermion fields e_R to the Higgs field Φ, recovers the invariance and gives the fermions their masses. Here, Y^e is the Yukawa coupling constant and $\bar{L}_L$ is the SU(2)$_L$ doublet. With the vev, this results in the mass term for the charged leptons and down-type quarks of $-m_e(\bar{e}_L e_R + \bar{e}_R e_L)$ with $m_e = \frac{Y^e v}{\sqrt{2}}$. With $\tilde{\Phi} = i\sigma_2 \Phi^*$, a similar Yukawa term can be written as $-Y^u \bar{L}_L \tilde{\Phi} u_R + h.c.$, which leads to the masses of the up-type quarks.

1.1.4 Leptonic Weak Interactions after Symmetry Breaking

After the spontaneous symmetry breaking, the leptonic part of the electroweak Lagrangian can be written as

$$\mathcal{L}_{\text{EW}}^{\ell} = \frac{g}{\sqrt{2}} W^+ \sum_{\alpha=e,\mu,\tau} \bar{\nu}_\alpha \gamma^\mu P_L \ell_\alpha + \frac{g}{4c_w} Z$$

$$\times \left\{ \sum_{\alpha=e,\mu,\tau} \bar{\nu}_\alpha \gamma^\mu P_L \nu_\alpha + \sum_\alpha \bar{\ell}_\alpha \gamma^\mu \left[2s_w^2 P_R - (1 - 2s_w^2) P_L \right] \ell_\alpha \right\} + h.c., \tag{1.11}$$

where $c_w \equiv \cos\theta_w$, $s_w \equiv \sin\theta_w$, P_L and P_R are the left and right projectors, respectively, while ν_α and ℓ_α, are the neutrino and charged lepton weak eigenstates. The W^+ and Z bosons are the massive gauge bosons of the weak interaction. The large boson masses $m_W \sim 80\,\text{GeV}$ and $m_Z \sim 90\,\text{GeV}$ result in a short range of the force of about 1×10^{-18} m. Interactions carried out by the $W^\pm$ bosons are called *charged current (CC)* interactions, as they propagate a charge, therefore changing the interacting lepton to its charged/neutral counterpart. *Neutral current (NC)* interactions are those mediated by the Z^0 boson, where no charge is transferred. NC interactions couple neutrinos to neutrinos and charged leptons to charged leptons, but not to each other. The Feynman diagrams for CC and NC interactions are shown in Figure 1.1.
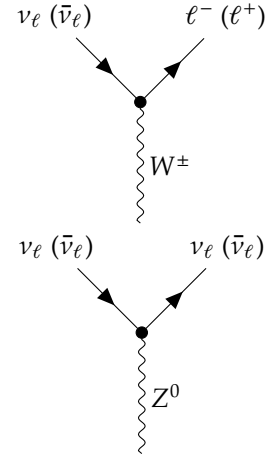
Figure 1.1: Feynman diagrams of charged-current (top) and neutral-current (bottom) neutrino weak interactions, modified from [13].

1.2 Beyond the Standard Model

The fundamentals of the SM described above **are not** enough to explain all observed phenomena. Gravity cannot be explained by the SM, as it is incompatible with general relativity, neither can some of the cosmological observations like *dark matter (DM)*, and the matter-antimatter asymmetry be explained. But most importantly, the SM does not predict neutrinos to

have mass, which is experimentally proven by neutrino oscillations, so some extension to the SM is needed in order to explain the observed phenomena.

Standard cosmology (ΛCDM) assumes that equal amounts of matter and anti-matter were produced in the early universe. However, the universe today is dominantly made up of matter. This so-called *baryon asymmetry of the universe (BAU)* can be measured by the difference between the number densities of baryons and anti-baryons normalized to the number density of photons as

$$\eta_B = \frac{n_B - n_{\bar{B}}}{n_\gamma} \, , \tag{1.12}$$

where n_B, $n_{\bar{B}}$, and n_γ are the number densities of baryons, anti-baryons, and photons, respectively. Baryons are the dominant component with η_B being observed to be around 6×10^{-10}. Leptogenesis and EW baryogenesis are scenarios that could explain this phenomenon, where the former could be realized by the existence of heavy RH neutrinos.

The observation of neutrino flavor conversions and neutrino oscillations in a multitude of experiments [14–16] is the strongest evidence for physics beyond the SM measured in laboratories to date. The observation that neutrinos change their flavor while they propagate through space can only be explained, if at least two neutrinos have a non-zero mass. From those measurements we know the mass differences are very small as compared to the lepton masses, but neither their existence, nor their smallness is predicted by the SM. There are upper limits on the sum of all neutrino masses from cosmological observations at 1.2 eV [17, 18] and at 0.8 eV from the KATRIN experiment [19]. Adding RH neutrino states to the theory could explain the origin of the observed non-zero neutrino masses and could be tested for by searching for corresponding signatures in experiments.

[14]: Davis et al. (1968), "Search for Neutrinos from the Sun"
[15]: Fukuda et al. (1998), "Evidence for Oscillation of Atmospheric Neutrinos"
[16]: Ahmad et al. (2002), "Direct Evidence for Neutrino Flavor Transformation from Neutral-Current Interactions in the Sudbury Neutrino Observatory"
[17]: Alam et al. (2021), "Completed SDSS-IV extended Baryon Oscillation Spectroscopic Survey: Cosmological implications from two decades of spectroscopic surveys at the Apache Point Observatory"
[18]: Aghanim et al. (2020), "Planck2018 results: VI. Cosmological parameters"
[19]: Aker et al. (2022), "Direct neutrino-mass measurement with sub-electronvolt sensitivity"

1.2.1 Mass Mechanisms

Since there are no RH neutrinos in the SM, the mass mechanism described in Section 1.1.3, which couples the Higgs field to LH and RH Weyl fields, predicts the LH neutrinos to be massless. From experimental observations it is known that at least two of the three neutrino generations need to have a non-zero mass. Assuming the existence of RH neutrinos fields ν_R, one way of producing the neutrino masses is by adding a Yukawa coupling term similar to the one for up-type quarks mentioned in Section 1.1.3, to write the full Yukawa Lagrangian as

$$\mathscr{L}_{\text{Yukawa}} = -Y_{ij}^e \bar{L}_L^i \Phi e_R^j - Y_{ij}^\nu \bar{L}_L^i \tilde{\Phi} \nu_R^j + h.c. \, , \tag{1.13}$$

with i, j running over the three generations of leptons e, μ, and τ, and Y^e and Y^ν being the Yukawa coupling matrices. Diagonalizing the Yukawa coupling matrices through unitary transformations U^e and U^ν leads to the **Dirac mass term** in the mass basis as

$$\mathscr{L}_{\text{Dirac}}^{\text{mass}} = \frac{v}{\sqrt{2}} \left(\bar{e}_L M_e e_R - \bar{\nu}_L M_\nu \nu_R \right) \, , \tag{1.14}$$

where M_e and M_ν are the diagonal mass matrices of leptons and neutrinos, respectively. A purely Dirac mass term would not explain the smallness of the neutrino masses in a straightforward way. Only fine-tuning the Yukawa coupling constants to small values would lead to small neutrino masses.

An additional way of generating neutrino masses is by adding a Majorana mass term of the form

$$\mathscr{L}_{\text{Majorana}} = -\frac{1}{2} M_{ij} (\nu_R^i)^c \nu_R^j + h.c. \, , \qquad (1.15)$$

with M_{ij} being the Majorana mass matrix and the indices i, j running over all n_R RH neutrino generations. The superscript c denotes the charge conjugate field. Combining the charge conjugated RH neutrino fields with the LH neutrino fields as

$$N = \begin{pmatrix} \nu_L \\ \nu_R^c \end{pmatrix} , \qquad (1.16)$$

with ν_R containing the n_R RH fields. The full neutrino mass Lagrangian is then given by the combined **Dirac and Majorana mass term** as

$$\mathscr{L}_{\text{Dirac+Majorana}}^{\text{mass},\nu} = \frac{1}{2} N^T \hat{C} M^{\text{D+M}} N + h.c. \, , \qquad (1.17)$$

and the mass matrix is given by

$$M^{\text{D+M}} = \begin{pmatrix} 0 & (M^D)^T \\ M^D & M^R \end{pmatrix} . \qquad (1.18)$$

On top of explaining the origin of neutrino masses itself, a combined Dirac and Majorana mass term could also solve the question of their smallness. If the mass of the RH neutrinos is very large, the masses of the active neutrino flavors is suppressed, which is known as *see-saw mechanism*.

1.2.2 Minimal Extensions and the νMSM

So far we have described neutrinos in their flavor eigenstates, which are relevant for weak interactions, where the three weak flavor states ν_e, ν_μ, and ν_τ are related to the charged leptons they interact with in CC interactions. In order to *just* explain the three oscillating flavor eigenstates, three mass states are needed, which are related to the flavor eigenstates by the unitary, 3x3 *Pontecorvo-Maki-Nakagawa-Sakata (PMNS)* mixing matrix U, where the flavor states are a superposition of the mass states as

$$|\nu_\alpha\rangle = \sum_k U_{\alpha k}^* |\nu_k\rangle \, , \qquad (1.19)$$

with the weak flavor states $|\nu_\alpha\rangle$, $\alpha = e, \mu, \tau$, and the mass states $|\nu_k\rangle$ with $k = 1, 2, 3$. In its generic form the PMNS matrix is given by

$$U = \begin{pmatrix} U_{e1} & U_{e2} & U_{e3} \\ U_{\mu 1} & U_{\mu 2} & U_{\mu 3} \\ U_{\tau 1} & U_{\tau 2} & U_{\tau 3} \end{pmatrix} , \qquad (1.20)$$

which will be the basis for the discussion of neutrino oscillations in Section 1.3.2.

This however is not enough to explain the neutrino masses observed in oscillation experiments. The most minimal model required to give rise to two non-zero active neutrino masses, is an additional two RH neutrinos, assuming the mass of the lightest SM neutrino is zero. If the additional neutrino states have masses $\gg$eV they are referred to as *heavy neutral leptons*

> add Majorana condition and mention what this means for interactions (LNV of 2) (ORANGE)

(HNL), which are almost sterile, with a small mass mixing with the active neutrinos.

But the SM also fails to explain additional observations of physics beyond the standard model (BAU, DM), which could be solved by the *neutrino minimal standard model (νMSM)* [20, 21]. In the νMSM, three RH neutrinos are added, where two of them are heavy, to explain the observed neutrino masses and oscillations, and a third one is light and serves as a DM candidate. The mixing between mass and flavor eigenstates is then described by an extended 6x6 mixing matrix as

[20]: Asaka et al. (2005), "The nuMSM, dark matter and neutrino masses"
[21]: Asaka et al. (2005), "The νMSM, dark matter and baryon asymmetry of the universe"

> elaborate on Leptogenesis in νMSM and sterile neutrino DM, or link some papers? (ORANGE)

$$\begin{pmatrix} \nu_e \\ \nu_\mu \\ \nu_\tau \\ N_1 \\ N_2 \\ N_3 \end{pmatrix} = \begin{pmatrix} U_{e1} & U_{e2} & U_{e3} & U_{e4} & U_{e5} & U_{e6} \\ U_{\mu1} & U_{\mu2} & U_{\mu3} & U_{\mu4} & U_{\mu5} & U_{\mu6} \\ U_{\tau1} & U_{\tau2} & U_{\tau3} & U_{\tau4} & U_{\tau5} & U_{\tau6} \\ U_{N_11} & U_{N_12} & U_{N_13} & U_{N_14} & U_{N_15} & U_{N_16} \\ U_{N_21} & U_{N_22} & U_{N_23} & U_{N_24} & U_{N_25} & U_{N_26} \\ U_{N_31} & U_{N_32} & U_{N_33} & U_{N_34} & U_{N_35} & U_{N_36} \end{pmatrix} \begin{pmatrix} \nu_1 \\ \nu_2 \\ \nu_3 \\ \nu_4 \\ \nu_5 \\ \nu_6 \end{pmatrix}, \tag{1.21}$$

where N_i and ν_{i+3} ($i \in [1, 2, 3]$) are the sterile flavor states and the additional RH states, respectively. In the νMSM, the two heavy RH neutrinos generate the active neutrino masses through the type I seesaw mechanism, where they are assumed to be SM scalars and couple to the Higgs field as such.

> add all the references here (RED)

1.2.3 Observational Avenues for Right-Handed Neutrinos

If the RH neutrinos have masses at the eV scale, they can be observed through distortion effects in measurements of neutrino oscillation experiments. Several analyses looking for light sterile neutrinos exit in IceCube, where [22] is using higher energies and [13] the lower energy part. The latter work includes a detailed description of the expected oscillation effects and the various anomalies observed in oscillation experiments that could be explained by the existence of a light sterile neutrino.

[22]: Aartsen et al. (2020), "An eV-scale sterile neutrino search using eight years of atmospheric muon neutrino1data from the IceCube Neutrino Observatory"
[13]: Trettin (2023), "Search for eV-scale sterile neutrinos with IceCube DeepCore"

For this work, the focus will be on heavy RH neutrinos, heavy sterile neutrinos, or HNLs, which are too massive to be produce in oscillations and to be observed there. Several ways to observe HNLs are possible through direct production and decay experiments, which will be discussed in the following. Most of the existing searches assume the minimal model, where only one coupling between the new mass states and the SM neutrinos is non-zero and the coupling is just through mass mixing in type I seesaw scenarios, but more complex scenarios are possible and might produce various signatures.

1.2.4 Searching for Heavy Neutral Leptons

Colliders

LHC: proton-proton collider sqrt(s): 7, 8, 13

ATLAS/CMS: nearly hermetic detectors around interaction, multiple searches for HNL scenarios LHCB: forward detector, designed to search for new particles in decays of heavy hadrons

Type I Seesaw Results:

HNL production in GeV reange from : decays of heavy mesons, tau leptons, W bosons, H bosons, or top quarks HNL decays: to lepton number conserving (dirac), or lepton number conserving and violating channels (majorana), depending on mass and mixing parameters, prompt and displaced decays are possible

Atlas results set constraints on mixing with e and mu:

Atlas in minimal extension: 10^-6 with $|U_{\mu 4}|^2$ at 4-10 GeV same for CMS: 10^-5 with $|U_{\mu 4}|^2$ and $|U_{e4}|^2$ at 10-600 GeV

CMS: final state of 3 leptons (two opposite charged and nu) giving $|U_{\mu 4}|^2$ $4 * 10^-7$ at 8-14 GeV

the above mentioned (strong) constraints are mostly based on a model with one HNl coupling to one flavor in type 1 seesaw at least 2 are needed to see the two SM nu masses, both coupling to several flavors it was shown (cite) that re-interpreting these results with more than one HNL can lead to much weaker constraints and to compare results, the assumed model and couplings have to be considered the strong reduction in constraints is due to the opening of new channels, to which the search may not be sensitive

more complex scenarios are possible and might produce various signatures, but are harder to measure: extended gauge symmetries, effective field theories

type III seesaw (HNL as SM EW triplets) can be observed as they are produced in pairs (no active-sterile mixing needed) and result in multi lepton states and high pt jets -> strong exclusion of masses below 790 GeV

LHCb: low mass and high mass results (above below mW), competitive in low mass

low mass channel: B+ -> mu+ N -> pi+ mu-, at order 10^-3 for $|U_{\mu 4}|^2$ at 0.5-3.5 GeV

high mass channel: W+ -> mu+ mu+-jet, at order 10^-3-10^-2 / 10^-4-10^-3 for $|U_{\mu 4}|^2$ at 5-50 GeV for LNC/LNV

there is a shit ton of future colliders and/or experiments at the LHC planned, that have sensitivities to HNLs.. think about which/how to discuss them

Nuclear Decay

novel approach to search for HNLs through energy-momentum conservation measurements in nuclear reactions

mixing of HNL with electon nu/nubar would cause irregularities, interpretable as limits in $|U_{e4}|^2$ and m4

Beta Decay   detect kinks in the energy spectra at $Q - m_4 c^2$

m4 probable between energy detection threshold and Q value of the decay

tritium 3H: Q=18.6 keV

planned analysis in KATRIN and TRISTAN (1 to 18 keV mass) projected statistical upper limits (95) around 10^{-7} $|U_{e4}|^2$ (but will need detector upgrades)

in Project 8 measure the absolute neutrino mass using cyclotron radiation emission spectroscopy (CRES), may also be able to search for HNLs

atmospheric argon 39Ar: Q=565keV

DUNE: massive LArTPCs at long baseline (1300km) accelerator nu (1GeV), measure ionization charge of 39Ar beta decays: projected sensitivity in 20kev to 450keV mass range for $|U_{e4}|^2$ at 10^{-7} (requires substantial trigger development), without more like 10^{-5}

Electron Capture   requires total energy-momentum reconstruction of non nu final states in electron capture

e capture: pure 2-body decay of recoiling atom and electron neutrino (mono energetic) measureing atom and associated de-excitation xray or auger electron, energy momentum conservation can be probed

separated non-zero missing mass peak would indicate HNL mixing with the electron neutrino/antineutrino

BeEST experiment: 100-850 keV mass, 7Be (Q=862keV), previous results at 10^{-4} $|U_{e4}|^2$, future sensitivity at 10^{-7} $|U_{e4}|^2$ after upgrades to the experiment

(proposed) HUNTER experiment: 20-300 keV mass (K-capture of 131Cs), "significantly improve current limits"

Reactor Searches   MeV masses (up to 12) at short baseline reactor experiments (commercial or research reactors)

source of electron antineutrinos, therefore also HNL (if they mix)

visible channels: N to nu e+ e-, and N to nu gamma, nu gamma gamma, where the first dominates

pioneering analysis reports 10^{-4} $|U_{e4}|^2$ at 2-7 MeV mass range

many experiments exist at 5-25 meters from reactor core, at 100 MW research or 1 GW commercial reactors and 1-5 m3 volume detectors.. these are designed to adress reactor anomaly, but could most likely also proble decay in flight to electron positron
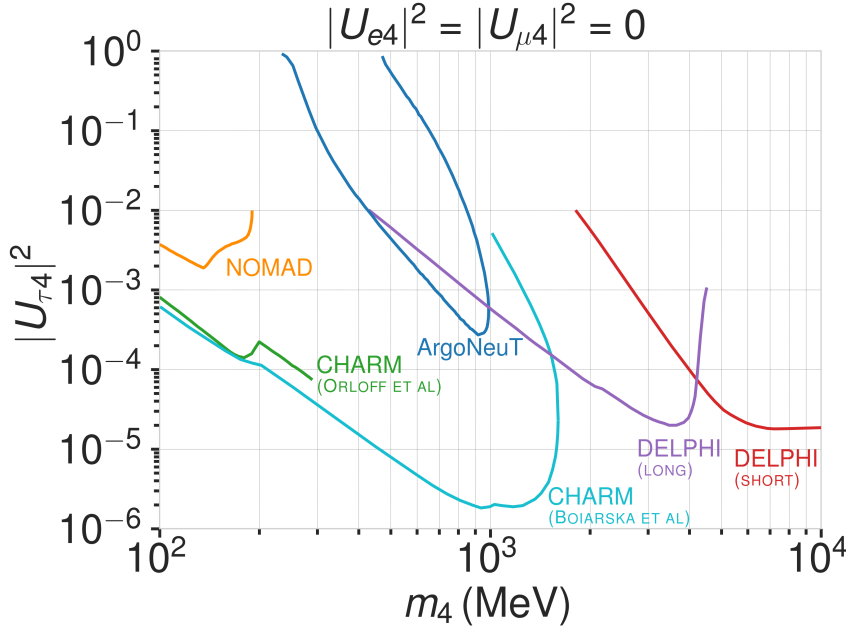
Figure 1.2: Current $|U_{\tau 4}^2| - m_4$ limits from NOMAD [23], ArgoNeut [24], CHARM [25, 26], and DELPHI [27].

Extracted Beamlines

protons interacting with a target or a beam dumb can produce pions, kaons, and heavy-quark hadrons, which can decay to neutrinos and HNLs

HNLs from those interactions can have energies of 1 MeV to 5 GeV and decay at long distances, because of their long lifetimes (model dependent)

experiments using a spectrometer with particle identification can detect unique decay signatures at displaced vertices

the observable signature is just a displaced vertex from for example N to l pi, N to l+ l-, N to nu pi0 etc., which cannot be explained by SM neutrinos, without scattering process (not sufficient mass)

depending on the decay channel, a specific mixing can be probed

the other way of searching for HNLs with this is to look for peaks in the missing mass spectrum at the production vertex (at target)

HNL search pioneer work was done by experiments at extracted beam lines, with early results from PS191, CHARM, NOMAD reporting bounds from direct production and decay of HNLs

today there is a large activity of searches for HNLs at extracted beamlines and the strongest bounds on decays are by recent results at PIENU [24, 25], NA62 [28, 29], T2K [36, 514], MicroBooNE [515, 516], and ArgoNeuT [517] experiments

as a standard, the results are presented with only one non-zero mixing parameter at a time

show strongest limits for all three mixings?

Atmospheric and Solar

natural sources of neutrinos up to 20 MeV (solar) and 100s of GeV (atmospheric)

both provide all flavors because of mixing/oscillations and can therefore be used to probe mixing with nu_e, $nu_m u$, and $nu_t au$

depending on the mass and mixing, which govern the decay length, different signatures can be used to probe large parts of the phase space

depending on the type of coupling (just mass-mixing, or more complicated like dipole-portal) considered, the scales could be different

Production in the Sun   if the HNL lifetimes are large enough, they could reach the detector after being produced in the sun

this will only allow production through non-zero $|U_{e4}|^2$ and not the other mixings

measurements of the decay to e+ e- nu and comparing to the expected inter-plenatry positron flux as was done in Borexino lead to the strongest limits in the few MeV regime

KAMLAND and Super-K could potentially also search for this through the inverse beta decay

Upscatter outside of the Detector   for HNL decay length scales of the order of the Earth's diameter, the HNLs could be upscattered anywhere in the earth from the solar or atmospheric neutrino fluxes and decay in the detector

for masses below 18 MeV, limits were derived in [37] R. Plestid (2020), 2010.04193 and [585] R. Plestid (2020), 2010.09523 (just tau-coupled for mixing and all flavor for dipole-portal) and decay in Borexino

in principle this could also be possible for atmospheric neutrinos, but flux and oscillation have to be taken into account

direct production of HNLs in the atmosphere is also possible, but has not been investigated yet

Production and Decay in the Detector   If HNL decay lengths are sufficiently short, production and decay could happen in the detector and the observation of two vertices could be used to constrain the mixing parameters

in principle mixing with any neutrino flavor produced in the sun or the atmosphere could be probed and theoretical studies have been performed for mass-mixing and dipole-portal couplings for IceCube and Super-K, Hyper-K, Dune

expand a bit more, or just jump to my section?

Cosmological and Astrophysical

leave these out for the moment?
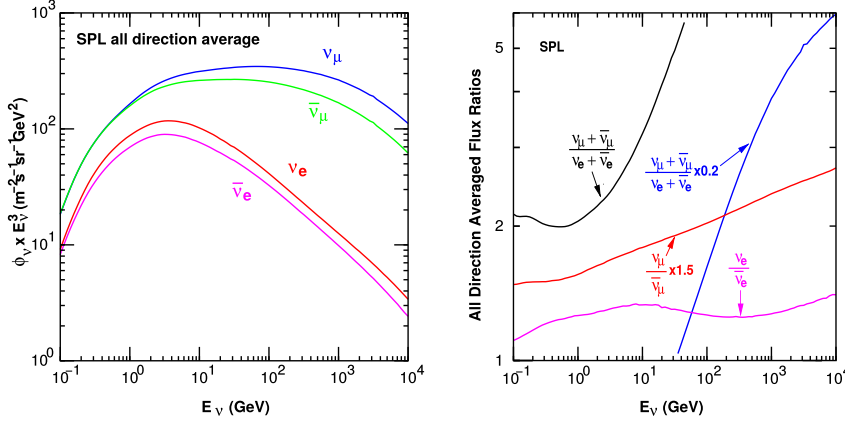
1.3 Atmospheric Neutrinos as Source of Heavy Neutral Leptons

1.3.1 Production of Neutrinos in the Atmosphere

The analysis performed in this work is based on the sample of neutrinos observed in IceCube DeepCore at energies below 100 GeV. At these energies, the flux exclusively originates in the Earth's atmosphere. Highly relativistic cosmic rays (protons and heavier nuclei [28]) interact in the upper atmosphere, producing showers of secondary particles. Neutrinos are produced in decays of charged pions and kaons (π and K mesons) present in those showers, where the dominant contribution comes from the decay chain

$$\pi^{\pm} \rightarrow \mu^{\pm} + \nu_{\mu}(\bar{\nu}_{\mu}) \, ,$$
$$\mu^{\pm} \rightarrow e^{\pm} + \bar{\nu}_{\mu}(\nu_{\mu}) + \nu_{e}(\bar{\nu}_{e}) \, , \tag{1.22}$$

where muon neutrinos ν_{μ} and muons $\mu^{\pm}$ are produced in the first decay and both electron and muon neutrinos $\nu_{e/\mu}$ are produced in the second decay. Atmospheric muons, which are also produced in these decays, are the main background component for IceCube DeepCore analyses.

The different atmospheric flux components are shown in Figure 1.3 (left), for a much broader energy range than relevant for this work. Both neutrinos and antineutrino fluxes are shown for electron and muon neutrinos and all fluxes are the directionally averaged expectation calculated at the South Pole. Muon neutrinos are dominating the flux and from Equation 1.22 the naive assumption would be that the ratio between muon and electron neutrinos is $(\nu_{\mu} + \bar{\nu}_{\mu})/(\nu_{e} + \bar{\nu}_{e}) = 2$. This is roughly true at energies below 1 GeV, where all muons decay in flight, but at larger energies muons can reach the detector before decaying, which increases the ratio to approximately 10:1 at around 100 GeV. Additionally, kaon decays start to contribute which also increases the number of muons and muon neutrinos. The increasing ratio can be seen in Figure 1.3 (right), which also shows the ration between neutrinos and antineutrinos for both flavors.

Charged mesons or tau particles can also be produced in cosmic ray interactions. Their decays lead to the production of tau neutrinos. At the energies relevant for this work however, the resulting tau neutrino flux is negligible as compared to the muon neutrino flux [30] and is not considered in the analysis. This is because both charged mesons and tau particles are much

heavier than pions and kaons and therefore their production is suppressed at high energies.

1.3.2 Oscillations

Describing neutrinos in their mass state as introduced in Section **??** is crucial to understand their propagation through space and time and to explain neutrino oscillations. Oscillations mean that a neutrino changes from its initial flavor, that it was produced with, to another flavor and back after traveling a certain distance.

The neutrino propagation in vacuum can be expressed by applying a plane wave approach, where the mass eigenstates evolve as

$$|\nu_k(t)\rangle = e^{-iE_k t/\hbar} |\nu_k\rangle \ . \tag{1.23}$$

The energy of the mass eigenstate $|\nu_k\rangle$ is $E_k = \sqrt{\vec{p}^2 c^2 + m_k^2 c^4}$, with momentum $\vec{p}$ and mass m_k, $\hbar$ is the reduced Planck constant, and c is the speed of light in vacuum. A neutrino is produced as a flavor eigenstate $|\nu_\alpha\rangle$ in a CC weak interaction, but its propagation happens as the individual mass states it is composed of. The probability of finding the neutrino with initial flavor $|\nu_\alpha\rangle$ in the flavor state $|\nu_\beta\rangle$ after the time t is calculated as

[31]: Dirac (1927), "The Quantum Theory of the Emission and Absorption of Radiation"

$$P_{\nu_\alpha \to \nu_\beta}(t) = | \langle \nu_\beta | \nu_\alpha(t) | \nu_\beta | \nu_\alpha(t) \rangle |^2 \ , \tag{1.24}$$

by applying Fermi's Golden Rule [31], which defines the transition rate from one eigenstate to another by the strength of the coupling between them. This coupling strength is the square of the matrix element and using the fact that the mixing matrix is unitary ($U^{-1} = U^\dagger$) to describe the mass eigenstates as flavor eigenstates, we find the time evolution of the flavor state $|\nu_\alpha(t)\rangle$, which can be inserted into Equation 1.24 to find the probability as

$$P_{\nu_\alpha \to \nu_\beta}(t) = \sum_{j,k} U_{\beta j}^* U_{\alpha j} U_{\beta k} U_{\alpha k}^* e^{-i(E_k - E_j)t/\hbar} \ . \tag{1.25}$$

The indices j and k run over the mass eigenstates.

We can approximate the energy as

$$E_k \approx E + \frac{c^4 m_k^2}{2E} \quad \longrightarrow \quad E_k - E_j \approx \frac{c^4 \Delta m_{kj}^2}{2E} \ , \tag{1.26}$$

for small neutrino masses compared to their kinetic energy. Here, $\Delta m_{kj}^2 = m_k^2 - m_j^2$ is the mass-squared splitting between states k and j. Replacing the time in Equation 1.25 by the distance traveled by relativistic neutrinos $t \approx L/c$ we get

$$P_{\nu_\alpha \to \nu_\beta}(t) = \delta_{\alpha\beta} - 4 \sum_{j>k} \mathbf{Re}(U_{\beta j}^* U_{\alpha j} U_{\beta k} U_{\alpha k}^*) \sin^2\left(\frac{c^3 \Delta m_{kj}^2}{4E\hbar} L\right)$$
$$+ 2 \sum_{j>k} \mathbf{Im}(U_{\beta j}^* U_{\alpha j} U_{\beta k} U_{\alpha k}^*) \sin^2\left(\frac{c^3 \Delta m_{kj}^2}{4E\hbar} L\right) \ , \tag{1.27}$$

which is called the survival probability if $\alpha = \beta$, and the transition probability if $\alpha \neq \beta$. Once again, this probability is only non-zero if there are neutrino mass eigenstates with masses greater than zero. Additionally, there must be a mass-squared difference Δm^2 and non-zero mixing between the states. Since we assumed propagation in vacuum in Equation 1.23, the transition and survival probabilities correspond to vacuum mixing.

The mixing matrix can be parameterized as [28]

$$U = \begin{pmatrix} 1 & 0 & 0 \\ 0 & c_{23} & s_{23} \\ 0 & -s_{23} & c_{23} \end{pmatrix} \begin{pmatrix} c_{13} & 0 & s_{13}e^{-i\delta_{CP}} \\ 0 & 1 & 0 \\ -s_{13}e^{i\delta_{CP}} & 0 & c_{13} \end{pmatrix} \begin{pmatrix} c_{12} & s_{12} & 0 \\ -s_{12} & c_{12} & 0 \\ 0 & 0 & 1 \end{pmatrix}, \quad (1.28)$$

where $c_{ij} = \cos \theta_{ij}$ and $s_{ij} = \sin \theta_{ij}$ are cosine and sine of the mixing angle θ_{ij}, that defines the strength of the mixing between the mass eigenstates i and j, and δ_{CP} is the neutrino CP-violating phase. Experiments are sensitive to different mixing parameters, depending on the observed energy range, neutrino flavor, and the distance between the source and the detector L, commonly referred to as *baseline*. To be able to resolve oscillations the argument

$$\frac{\Delta m^2 L}{4E} \quad (1.29)$$

should be at the order of 1. This divides experiments into ones that are sensitive to very slow oscillations from $\Delta m_{21}^2 \approx \mathcal{O}(10^{-5}\text{eV}^2)$ and ones that are sensitive to faster oscillations from $\Delta m_{31}^2 \approx \mathcal{O}(10^{-3}\text{eV}^2)$. Relevant for this work are the parameters that can be measured at the earths surface using atmospheric neutrinos, which are Δm_{31}^2, θ_{23}, and θ_{13}, because the flux is primarily composed of muon neutrinos and antineutrinos. Applying the parameterization from Equation 1.28 to Equation 1.27 and using the fact that θ_{13} is small and θ_{12} is close to $\pi/4$, the survival probability of muon neutrinos can be approximated as

$$\begin{aligned} P_{\nu_\mu \to \nu_\mu} &\simeq 1 - 4|U_{\mu3}|^2(1 - |U_{\mu3}|^2)\sin^2\left(\frac{\Delta m_{31}^2 L}{4E}\right) \\ &\simeq 1 - \sin^2\left(2\theta_{23}\right)\sin^2\left(\frac{\Delta m_{31}^2 L}{4E}\right), \end{aligned} \quad (1.30)$$

while the tau neutrino appearance probability is

$$\begin{aligned} P_{\nu_\mu \to \nu_\tau} &\simeq 4|U_{\mu3}|^2|U_{\tau3}|^2\sin^2\left(\frac{\Delta m_{31}^2 L}{4E}\right) \\ &\simeq \sin^2\left(2\theta_{23}\right)\sin^2\left(\frac{\Delta m_{31}^2 L}{4E}\right). \end{aligned} \quad (1.31)$$

The latest global fit [32] of all the parameters is shown in Table 1.2.

1.3.3 Interactions with Nuclei

The neutrino detection principle of IceCube DeepCore is explained in Chapter **??** and relies on the weak interaction processes between neutrinos and the nuclei of the Antarctic glacial ice. At neutrino energies above 5 GeV, the cross-sections are dominated by **deep inelastic scattering (DIS)**, where the neutrino is energetic enough to resolve the underlying structure of the nucleons and interact with one of the composing quarks individually. As a

adjust margintable vertical position (RED)

[28]: Tanabashi et al. (2018), "Review of Particle Physics"

Parameter	Global Fit
θ_{12} [°]	$33.41^{+0.75}_{-0.72}$
θ_{13} [°]	$8.54^{+0.11}_{-0.12}$
θ_{23} [°]	$49.1^{+1.0}_{-1.3}$
Δm_{21}^2 [10^{-5}eV^2]	$7.41^{+0.21}_{-0.20}$
Δm_{31}^2 [10^{-3}eV^2]	$2.511^{+0.028}_{-0.027}$
δ_{CP} [°]	197^{+42}_{-25}

Table 1.2: Results from the latest global fit of neutrino mixing parameters from [32].

[32]: Esteban et al. (2020), "The fate of hints: updated global analysis of three-flavor neutrino oscillations"

say something about matter effect? (ORANGE)

say something about mass ordering? (OR-ANGE)

result the nucleon breaks and a shower of hadronic secondary particles is produced. Depending on the type of interaction, the neutrino either remains in the final state for NC interactions or is converted into its charged lepton counterpart for CC interactions. The CC DIS interactions have the form

$$\nu_l + N \rightarrow l^- + X ,$$
$$\bar{\nu}_l + N \rightarrow l^+ + X ,$$

(1.32)

where $\nu_l/\bar{\nu}_l$ and l^-/l^+ are the neutrino/antineutrino and its corresponding lepton/antilepton, and l can be either an electron, muon, or tau. N is the nucleon and X stands for any set of final state hadrons. The NC DIS interactions are

$$\nu_l + N \rightarrow \nu_l + X \text{ and}$$
$$\bar{\nu}_l + N \rightarrow \bar{\nu}_l + X .$$

(1.33)

Figure 1.4 shows the Feynman diagrams for both processes DIS interactions

Figure 1.4: Feynman diagrams for deep inelastic scattering of a neutrino with a nucleon via charged-current (left) and neutral current (right) interactions. $\boldsymbol{p}_{\nu_i}$, $\boldsymbol{p}_N$ and $\boldsymbol{p}_{\nu_f}$, $\boldsymbol{p}_l$, $\boldsymbol{p}_N$ are the input and output four-momenta, while $\boldsymbol{q}$ is the momentum transfer. Taken from [33].
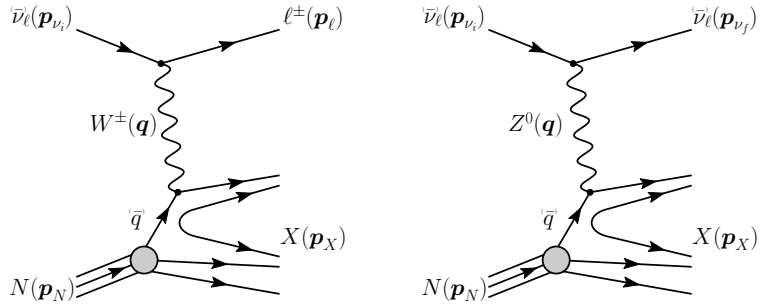
have a roughly linear energy dependent cross-section above ∼20 GeV and are well measured and easy to theoretically calculate. They are the primary interaction channel for neutrinos detected with IceCube.

At energies below 5 GeV, *quasi-elastic scattering (QE)* and *resonant scattering (RES)* become important. At these energies the neutrinos interact with the approximately point-like nucleons, without breaking them up in the process. RES describes the process of a neutrino scattering off a nucleon producing an excited state of the nucleon in addition to a charged lepton. It is the dominant process at 1.5 GeV to 5 GeV for neutrinos and 1.5 GeV to 8 GeV for antineutrinos. Below 1.5 GeV QE is the main process, where protons are converted to neutrons in antineutrino interactions and vice-versa for neutrino interactions. Additionally, a charged lepton corresponding to the neutrino/antineutrino flavor is produced. The cross-sections of QE and RES scattering processes are not linear in energy and the transition region from QE/RES to DIS is poorly understood. The total cross-sections and their composition is shown in Figure 1.5. It can be seen that the interaction cross-sections are very small at the order of 10^{-38} cm^2. This is the reason why very large volume detectors are required to measure atmospheric neutrinos with sufficient statistics to perform precision measurements of their properties. The interaction length of a neutrino with $E_\nu = 10$ GeV is of $\mathcal{O}(10 \times 10^{10}$ km$)$, for example.
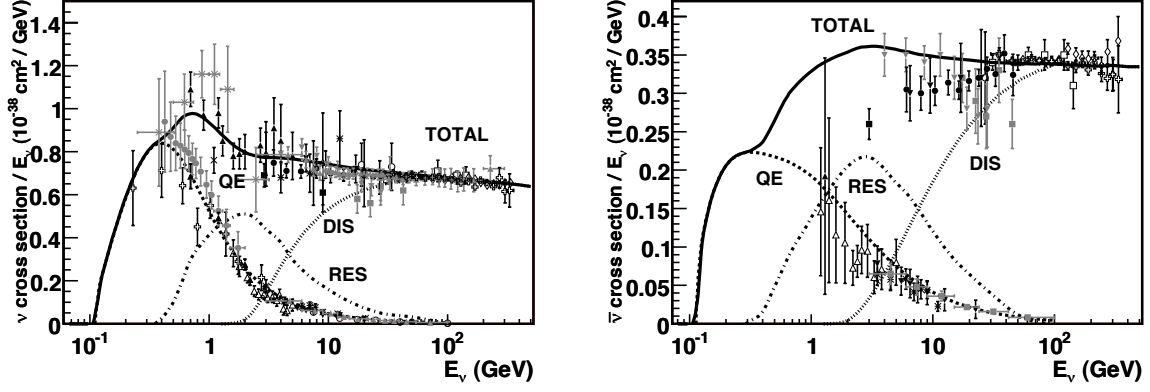
Figure 1.5: Total neutrino (left) and antineutrino (right) per nucleon cross-section divided by neutrino energy plotted against energy. The three main scattering processes quasi-elastic scattering (QE), resonant scattering (RES), and deep-inelastic scattering (DIS) are shown. Taken from [34].
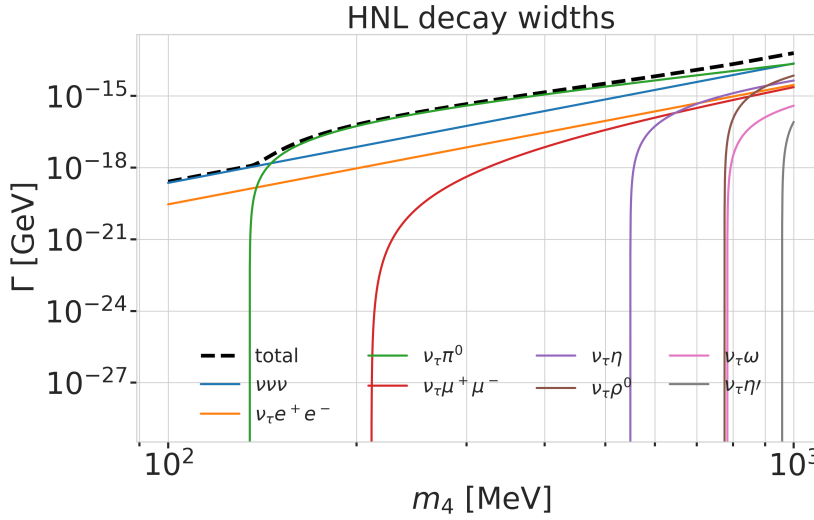
Figure 1.6: Decay widths of the HNL within the mass range considered, calculated based on the results from [35]. Given the existing constraints on $|U_{e4}|^2$ and $|U_{\mu4}|^2$, we consider that the corresponding decay modes are negligible.

HNL Production and Decay

Up-Scattering in the Ice

Decay in the Ice

Re-write/re-formulate this section (copied from HNL technote). (RED)

[35]: Coloma et al. (2021), "GeV-scale neutrinos: interactions with mesons and DUNE sensitivity"

To explain the signature we can observe in IceCube we first have to revisit the weak interactions that the HNL inherits from its LH counterpart through mixing. We will be following the derivation in [35]. Extending the SM by n additional RH neutrinos, ν_i ($i = 3 + n$), leads to the mass Lagrangian

$$\mathscr{L}_\nu^{mass} \supset - \sum_{\alpha=e,\mu,\tau} \sum_{i=4}^{3+n} Y_{\nu,\alpha i} \overline{L}_{L,\alpha} \tilde{\phi} \nu_i - \frac{1}{2} \sum_{i=4}^{3+n} M_i \overline{\nu}_i \nu_i^c + h.c., \qquad (1.34)$$

in a basis where the Majorana mass terms are diagonal. $Y_{\nu,\alpha i}$ are the Yukawa couplings to the lepton doublets and M the Majorana masses for the heavy singlets. $L_{L,\alpha}$ stands for the SM LH lepton doublet of flavor α while ϕ is the Higgs field, and $\tilde{\phi} = i\sigma_2 \phi^*$ and $\nu_i^c \equiv C\overline{\nu}_i^t$, with $C = i\gamma_0\gamma_2$ in the Weyl representation. The full neutrino mass matrix with the Higgs vacuum

expectation value $v/\sqrt{2}$ reads

$$\mathcal{M} = \begin{pmatrix} 0_{3\times3} & Y_\nu v/\sqrt{2} \\ Y_\nu^t v/\sqrt{2} & M \end{pmatrix}, \tag{1.35}$$

and can be diagonalized by a $(3+n)$ x $(3+n)$ full unitary roation U, that itself leads to neutrino masses upon diagonalization, additionally manifesting the mixing between active neutrinos and heavy states. The resulting model consists of 3 light SM neutrino mass eigenstates ν_i ($i = 1, 2, 3$) and n heavier states, as introduced above. The flavor states will now consist of a combination of light and heavy states

$$\nu_\alpha = \sum_{i=1}^{3+n} U_{\alpha i} \nu_i, \tag{1.36}$$

and the leptonic part of the EW Lagrangian can be written as

$$\mathcal{L}_{\text{EW}}^\ell = \frac{g}{\sqrt{2}} W_\mu^+ \sum_\alpha \sum_i U_{\alpha i}^* \bar{\nu}_i \gamma^\mu P_L \ell_\alpha + \frac{g}{4 c_w} Z_\mu$$

$$\times \left\{ \sum_{i,j} C_{ij} \bar{\nu}_i \gamma^\mu P_L \nu_j + \sum_\alpha \bar{\ell}_\alpha \gamma^\mu \left[2 s_w^2 P_R - (1 - 2 s_w^2) P_L \right] \ell_\alpha \right\} + h.c., \tag{1.37}$$

while

$$C_{ij} \equiv \sum_\alpha U_{\alpha i}^* U_{\alpha j}. \tag{1.38}$$

The indices now sum over all $(3 + n)$ flavor and mass states.

Based on this formulation and assuming that only the mixing with the tau sector is open ($|U_{\alpha 4}^2| = 0, \alpha = e, \mu$), the relevant production diagram of the HNL can be drawn as shown in Figure **??**. Alongside the fourth heavy mass state, a Hadronic cascade is produced. The heavy mass state will travel for some distance (dependent on mass and mixing) before it decays. The subsequent decay processes are depicted in Figure **??**. It can be a CC or NC decay and both leptonic and mesonic modes are possible (dependent on the mass). This will produce a tau or a tau neutrino and another cascade that can be EM or Hadronic. The branching ratios corresponding to the decay modes of the HNL for the mass range of interest (i.e. between 100 MeV and 1 GeV) are shown in Figure **??** as a function of the HNL mass.

Search for Tau Neutrino Induced Heavy Neutral Lepton Events

2

This chapter describes the search for HNL events using 10 years of IceCube DeepCore data. The expected number of HNL events in the data sample depends on the mass of the additional heavy state, m_4, and the mixing element $|U_{\alpha 4}^2|$, with $\alpha = e, \mu, \tau$, between the SM flavors and the new mass state. As discussed in Section 1.3, this work focuses on the mixing to the tau sector, $|U_{\tau 4}^2|$, which has the weakest constraints to date. Since the mass itself influences the production and decay kinematics of the event and the accessible decay modes, individual mass samples were produced as described in Section **??**. The mass influences the decay length and energy distributions, while the mixing both changes the overall expected rate of the HNL events and the shape in energy and length. We perform three independent searches for each mass sample, where the mixing is measured in each of the fits.

2.1 Final Level Sample

The final level simulation sample of this analysis consists of the neutrino and muon MC introduced in Section **??** and one of the three HNL samples explained in Section **??**, while the data are the events measured in 10 years of IceCube DeepCore data taking. All simulation and the data are processed through the full event selection chain described in Section **??** and Section **??** leading to the final level sample. As described in Section **??**, event triggers consisting purely of random coincidences induced by noise in the DOMs have been reduced to a negligible rate, and will not be discussed further.

To get the neutrino expectation, the MC events are weighted according to their generation weight introduced in Section **??**, multiplied by the total lifetime, and the expected neutrino flux. For the correct expectation at the detector, the events have to be weighted by the oscillation probability, depending on their energy and their distance traveled from the atmosphere to the detector. The oscillation probabilities are calculated using a PYTHON implementation of the calculations from [36], which use the matter profile of the Earth following the *Preliminary Reference Earth Model (PREM)* [37] as input. Apart from the energy and the distance, the two relevant parameters defining the oscillation probabilities are the atmospheric neutrino oscillation parameters θ_{23} and Δm_{31}^2. Since the HNL events originate from the tau neutrinos that were produced as muon neutrinos in the atmosphere and then oscillated into ν_τ, this weighting is also applied in addition to the specific weighting scheme for the HNL events described in Section **??**, which itself is defined by the mixing $|U_{\tau 4}^2|$ and the mass m_4.

[36]: Barger et al. (1980), "Matter effects on three-neutrino oscillations"
[37]: Dziewonski et al. (1981), "Preliminary reference Earth model"

2.1.1 Expected Rates/Events

The rates and the expected number of events for the SM background are shown in Table 2.1 with around 175000 total events expected in the 10 years. Only data marked as good is used for the analysis, where *good* refers to

measurement time with the correct physics run configuration and without other known issues. The resulting good detector livetime in this data taking period was 9.28 years. The rates are calculated by summing the weights of all events in the final level sample, while the uncertainties are calculated by taking the square root of the sum of the weights squared. The expected number of events is calculated by multiplying the rate with the livetime. The individual fractions show that this sample is neutrino dominated where the majority of events are ν_μ-CC events.

Table 2.1: Final level rates and event expectation of the SM background particle types.

Type	Rate [mHz]	Events (9.28 years)	Fraction [%]
ν_μ^{CC}	0.3531	103321 ± 113	58.9
ν_e^{CC}	0.1418	41490 ± 69	23.7
ν_{NC}	0.0666	19491 ± 47	11.1
ν_τ^{CC}	0.0345	10094 ± 22	5.8
μ_{atm}	0.0032	936 ± 15	0.5
total	0.5992	175332 ± 143	100.0

Table 2.2 shows the rates and expected number of events for the HNL signal simulation. The expectation depends on the mass and the mixing and shown here are two example mixings for all the three masses that are being tested in this work. A mixing of 0.0 would result in no HNL events at all. It can already be seen that for the smaller mixing of $|U_{\tau 4}|^2 = 10^{-3}$ the expected number of events is very low, while at the larger mixing of $|U_{\tau 4}|^2 = 10^{-1}$ the number is comparable to the amount of atmospheric muons in the background sample.

Table 2.2: Final level rates and event expectations of the HNL signal for all three masses and two example mixing values.

HNL mass	Rate [µHz]	Events (in 9.28 years)
$|U_{\tau 4}|^2 = 10^{-1}$		
0.3 GeV	3.3	975 ± 2
0.6 GeV	3.1	895 ± 2
1.0 GeV	2.5	731 ± 2
$|U_{\tau 4}|^2 = 10^{-3}$		
0.3 GeV	0.006	1.67 ± 0.01
0.6 GeV	0.022	6.44 ± 0.01
1.0 GeV	0.025	7.27 ± 0.01

add 3D data histograms (RED)

Add fractions of the different particle types in the bins for benchmark mass/mixing (another table?) (ORANGE)

[38]: Yu et al. (2023), "Recent neutrino oscillation result with the Ice-Cube experiment"

link this to the BG 3-d histogram if I add it? (ORANGE)

fix caption (RED)

remake without the top row of masked bins? add label to cbar and remove from title (RED)

2.1.2 Analysis Binning

An identical binning to the analysis performed in [38] is used. In total, there are three bins in PID (cascade like, mixed, and track like), 12 bins in reconstructed energy, and 8 bins in cosine of the reconstructed zenith angle as specified in Table 2.3. Extending the binning towards lower energies or increasing the number of bins in energy or cosine of the zenith angle did not improve the HNL sensitivities significantly, because the dominant signal region is already covered with a sufficiently fine binning to observe the shape and magnitude of the HNL events. This can be seen in the middle panel of Figure 2.1.

Some low energy bins in the cascade like region have very low MC expectations (<1 event) and are therefore not taken into account in the analysis, to prevent unwanted behavior in the fit. Those are shown in dark green in the three dimensional histogram.

Variable	N_{bins}	Edges	Spacing
P_ν	3	[0.00, 0.25, 0.55, 1.00]	linear
E	12	[5.00, 100.00]	logarithmic
$\cos(\theta)$	8	[-1.00, 0.04]	linear

Table 2.3: Three dimensional binning used in the analysis. All variables are from the FLERCNN reconstruction explained in Section **??**.
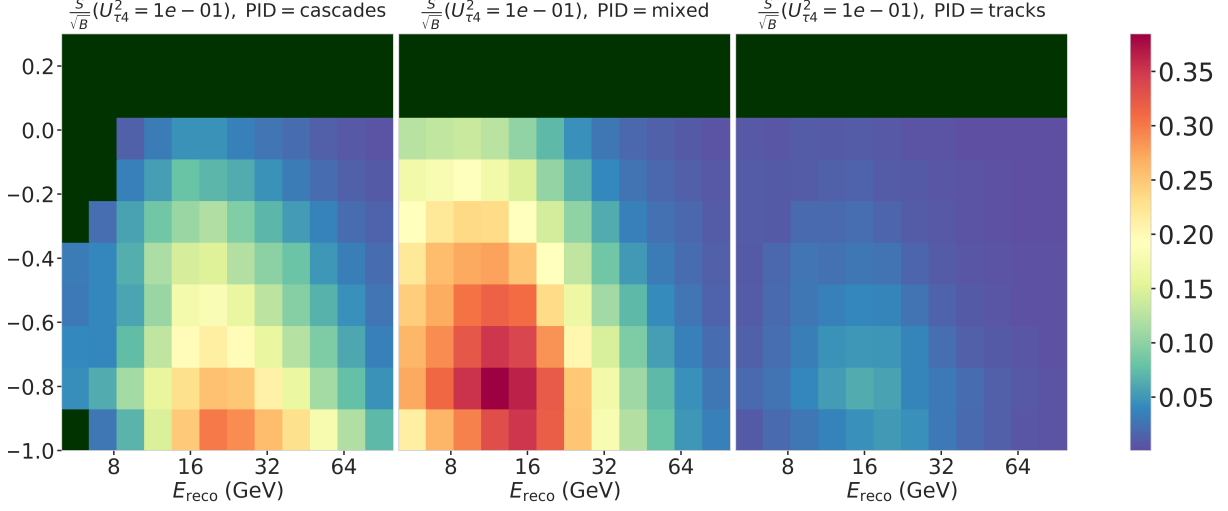

Figure 2.1

2.2 Statistical Analysis

2.2.1 Test Statistic

The measurements are performed by comparing the weighted MC to the data. Through variation of the nuisance and physics parameters that govern the weights, the best matching set of parameters can be found, by optimizing a fit metric. The comparison is done using a modified χ^2, defined as

$$\chi^2_{\text{mod}} = \sum_{i \in \text{bins}} \frac{(N_i^{\text{exp}} - N_i^{\text{obs}})^2}{N_i^{\text{exp}} + (\sigma_i^\nu)^2 + (\sigma_i^\mu)^2 + (\sigma_i^{\text{HNL}})^2} + \sum_{j \in \text{syst}} \frac{(s_j - \hat{s}_j)^2}{\sigma_{s_j}^2} \,, \qquad (2.1)$$

as the fit metric. It is designed such that taking the difference between a free fit and a fit with fixed parameters based on a chosen hypothesis, $\Delta\chi^2_{\text{mod}}$, can directly be used as a *test statistic (TS)* for hypothesis testing, due to its asymptotic behavior. The total even expectation is $N_i^{\text{exp}} = N_i^\nu + N_i^\mu + N_i^{\text{HNL}}$, where N_i^ν, N_i^μ, and N_i^{HNL} are the expected number of events in bin i from neutrinos, atmospheric muons, and HNLs, while N_i^{obs} is the observed number of events in the bin. The expected number of events from each particle type is calculated by summing the weights of all events in the bin $N_i^{\text{type}} = \sum_i^{\text{type}} \omega_i$, with the statistical uncertainty being $(\sigma_i^{\text{type}})^2 = \sum_i^{\text{type}} \omega_i^2$. The additional term in Equation 2.1 is included to apply a penalty term for prior knowledge of the systematic uncertainties of the parameters where they are known. s_j are the systematic parameters that are varied in the fit, while $\hat{s}_j$ are their nominal values and σ_{s_j} are the known uncertainties.

2.2.2 Physics Parameters

The variable physics parameter in this analysis is the mixing between the HNL and the SM τ sector, $|U_{\tau 4}|^2$. It is varied continuously in the range of [0.0 , 1.0] by applying the weighting scheme described in Section **??**. The fit is initialized at an off-nominal value of 0.1. The other physics parameter, the mass m_4 of the HNL, is implicitly fixed to one of the three discrete masses to be tested, by using the corresponding sample of the HNL simulation described in Section **??**.

2.2.3 Nuisance Parameters

interlude ...

Treatment of Detector Systematic Uncertainties

Since the variations related to the detector calibration uncertainties introduced in Section **??** are estimated by simulating MC at discrete values of the systematic parameters, a method to derive continuous variations is needed to perform the fit. The method applied here was initially introduced in [39] and first used in the low energy sterile neutrino search in [13] (section 7.4.3). Using a *likelihood-free inference* technique, re-weighting factors are found for every event in the nominal MC sample, given a specific choice of detector systematic parameters. These factors quantify how much more or less likely the event would be for the corresponding change in detector response from the nominal parameters. Without going into the details of the method, which were already exhaustively discussed in [39] and [13], the performance is assessed here for the HNL signal simulation. In order to do so, the weights are applied to the nominal MC samples, choosing the detector systematic values used to produce the discrete samples and the resulting event expectations are compared to the expectations from the individual, discrete MC samples. The bin counts are compared by calculating the pull defined as

$$ p = \frac{N_{\text{reweighted}} - N_{sys}}{\sqrt{\sigma^2_{\text{reweighted}} + \sigma^2_{sys}}} \, , \tag{2.2} $$

where N are the bin-wise event expectations and σ are their MC uncertainty. For the SM BG simulation, the performance was already investigated in [40] (section 7.4.4, appendix B5) and the re-weighted nominal MC was shown to be in agreement with the discrete systematic sets at a sufficient level. Figure **??** shows the bin-wise pulls for the 1.0 GeV HNL mass sample at a mixing of 0.1 for a selection of the discrete systematic samples, where the DOM efficiency and the bulk ice absorption was varied by ±10%. The distributions should follow a standard normal distribution, and no strong clustering or systematic deviations. It can be seen that spread of the distribution is slightly larger than 1.0 and the center is close to 0.0 as expected. A similar performance is found for the additional systematic sets and can be found in Section **??**.

[39]: Fischer et al. (2023), "Treating detector systematics via a likelihood free inference method"

[13]: Trettin (2023), "Search for eV-scale sterile neutrinos with IceCube DeepCore"

[40]: Lohfink (2023), "Testing non-standard neutrino interaction parameters with IceCube-DeepCore"

add bin-wise pulls and pull distribution for selection of sets and rest to backup (RED)

SB: generally you are missing a lot of references, and I don't think its very nice to read all these ranges and so on in the text. Surely you can just have a table with the systematics you include, their allowed range and prior if applicable? You can choose whether or not you want to discuss some parameters in more detail here, but it should be a discussion of the physics and impact on the analysis. e.g. you can include some plots showing how a change in some of the nuisance parameters changes the event counts in the analysis binning (RED)
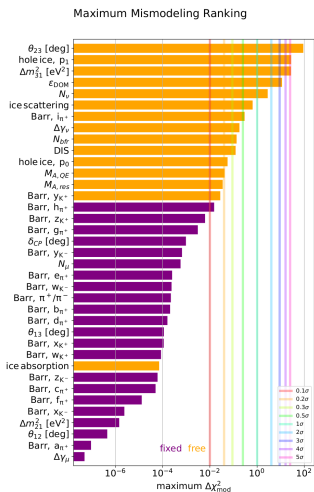

Figure 2.2: "calculated at a mixing of 0.1 and for the 1.0 GeV sample"

Free Parameters

To decide which systematic uncertainties should be included in the fit, we test the potential impact they have on the TS if they are neglected. The test is performed by creating Asimov data using the BG simulation and the HNL simulation of the 1.0 GeV mass sample at a mixing value of 0.1, which is chosen as a benchmark physics parameter, but the explicit choice does not have a significant impact on the test. The systematic parameter of interest is set to a value above its nominal expectation, either pulled up by $+1\sigma$ or by an educated estimate for parameters without a well-defined uncertainty. A fit is performed fixing the systematic parameter of interest and leaving all additional parameters free. The resulting TS is the mis-modeling significance between this fit and a fit with all parameters free, which would result in a TS of 0.0 for this Asimov test. Parameters below a significance of 0.1σ are fixed, and the test is performed in an iterative manner until the final set of free parameters is found.

Figure 2.2 shows the resulting significances of one of these tests. The parameters tested are the systematic parameters introduced in Section **??** and the atmospheric oscillation parameters mentioned in Section 2.1. In the final selection of free parameters the Barr h_{π^+} parameter was also left free and the ice absorption is still kept free, despite showing a small significance. This is done because the bulk ice parameters are not well constrained and are known to have a large impact, which might be concealed in this idealized test, due to correlations with the other parameters. In this test, the effect of correlations is challenging to consider, because only the impact of one parameter is tested at a time, using the overall mis-modeling significance as a measure. The mis-modeling could be reduced by a correlated parameter capturing the effect of the parameter of interest. For this reason a very conservative threshold of 0.1σ is chosen and some parameters below the threshold are still left free in the fit.

All nuisance parameters that are left free in the fit are summarized in Table 2.4, showing their nominal values, the allowed fit ranges, and their Gaussian prior, if applicable. The scaling parameter N_ν is included to account for the overall normalization of the neutrino rate, and it has the identical effect on the SM neutrino events and the BSM HNL events, because they both originate from the same neutrino flux. Despite being known to ~5 % in this energy range, there is no prior applied to this parameter, because the fit itself is able to constrain it well, which can be seen by the large impact it shows in Figure 2.2. Concerning the atmospheric neutrino flux, the CR power law flux correction factor $\Delta\gamma_\nu$ introduced in Section **??** is included with nominal value of 0.0 which corresponds to the baseline flux model by Honda *et al* [29]. A slightly conservative prior of 0.1 is applied to the parameter, while latest measurements show an uncertainty of 0.05 [41].

All the detector systematic uncertainties discussed in Section **??** are included in the fit. The DOM efficiency ϵ_{DOM} is constrained by a Gaussian prior with a width of 0.1, which is a conservative estimate based on the studies of the optical efficiency using minimum ionizing muons from [42, 43].

The two atmospheric neutrino oscillation parameters θ_{23} and Δm_{31}^2 are also included in the fit with nominal values of 47.5° and 2.48×10^{-3} eV^2 [38], respectively. Since they govern the shape and the strength of the tau neutrino

---

Blow up labels/legend/title and make it more readable in the margin or move it into the main text? (RED)

elaborate why this is also done to cover the whole energy range for the Pion production, referencing the Barr Block plot that I haven't included yet :D (RED)

Need cite here! (RED)

[29]: Honda et al. (2015), "Atmospheric neutrino flux calculation using the NRLMSISE-00 atmospheric model"

[41]: Evans et al. (2017), "Uncertainties in atmospheric muon-neutrino fluxes arising from cosmic-ray primaries"

[42]: Feintzeig (2014), "Searches for Point-like Sources of Astrophysical Neutrinos with the IceCube Neutrino Observatory"

[43]: Kulacz (2019), "In Situ Measurement of the IceCube DOM Efficiency Factor Using Atmospheric Minimum Ionizing Muons"

[38]: Yu et al. (2023), "Recent neutrino oscillation result with the IceCube experiment"

Table 2.4: Systematic uncertainty parameters that are left free to float in the fit. Their allowed fit ranges are shown with the nominal value and the Gaussian prior width if applicable.

Parameter	Nominal	Range	Prior
$\theta_{23}[°]$	47.5047	[0.0, 90.0]	-
$\Delta m_{31}^2[eV^2]$	0.002475	[0.001, 0.004]	-
N_ν	1.0	[0.1, 2.0]	-
$\Delta\gamma_\nu$	0.0	[-0.5, 0.5]	0.1
Barr h_{π^+}	0.0	[-0.75, 0.75]	0.15
Barr i_{π^+}	0.0	[-3.05, 3.05]	0.61
Barr y_{K^+}	0.0	[-1.5, 1.5]	0.3
DIS	0.0	[-0.5, 1.5]	1.0
$M_{A,QE}$	0.0	[-2.0, 2.0]	1.0
$M_{A,res}$	0.0	[-2.0, 2.0]	1.0
ϵ_{DOM}	1.0	[0.8, 1.2]	0.1
hole ice p_0	0.101569	[-0.6, 0.5]	-
hole ice p_1	-0.049344	[-0.2, 0.2]	-
bulk ice absorption	1.0	[0.85, 1.15]	-
bulk ice scattering	1.05	[0.9, 1.2]	-
N_{bfr}	0.0	[-0.2, 1.2]	-

flux, by defining the oscillation from ν_μ to ν_τ, they are also relevant for the HNL signal shape.

I should add some final level effects of some systematics on the 3D binning and maybe discuss how they are different from the signal shape, or so? (ORANGE)

[44]: Aartsen et al. (2020), "Computational techniques for the analysis of small signals in high-statistics neutrino oscillation experiments"

2.2.4 Low Energy Analysis Framework

The analysis is performed using the PISA [44] [45] software framework, which was developed to perform analyses of small signals in high-statistics neutrino oscillation experiments. It is used to generate the expected event distributions from several MC samples, which can then be compared to the observed data. The expectation for each MC sample is calculated by applying physics and nuisance parameter effects in a stage-wise manner, before combining them to the final expectation.

2.3 Analysis Checks

[46]: Nickerson (1998), "Confirmation Bias: A Ubiquitous Phenomenon in Many Guises"

Fitting to data is performed in a *blind* manner, where the analyzer does not immediately see the fitted physics and nuisance parameter values, but first checks that a set of pre-defined *goodness of fit (GOF)* criteria are fulfilled. This is done to circumvent the so-called *confirmation bias* [46], where the analyzer might be tempted to construct the analysis in a way that confirms their expectation. After the GOF criteria are met to satisfaction, the fit results are unblinded and the full result can be revealed. Before these blind fits to data are performed, the robustness of the analysis method is tested using pseudo-data that is generated from the MC.

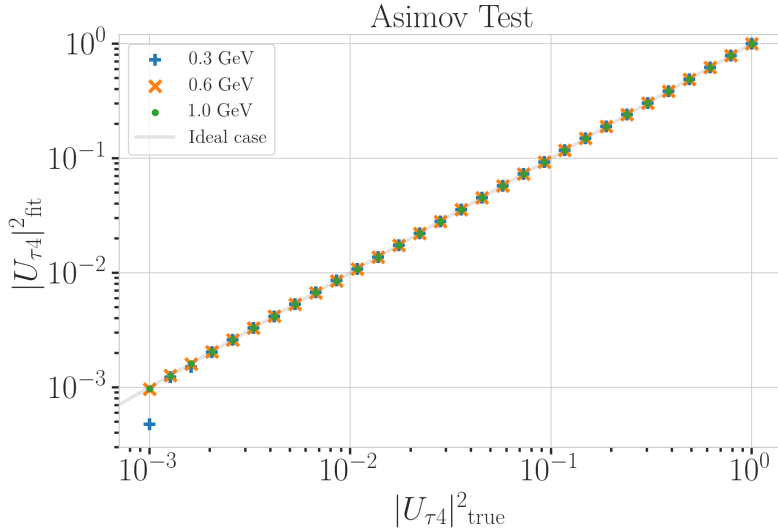### 2.3.1 Minimization Robustness

1: There is a degeneracy between the lower octant ($\theta_{23} < 45°$) and the upper octant ($\theta_{23} > 45°$), which can lead to fit metric minima (local and global) at two positions that are mirrored around 45° in θ_{23}.

[47]: Dembinski et al. (2022), *scikit-hep/iminuit: v2.17.0*

To find the set of parameters that best describes the data, a staged minimization routine is used. In the first stage, a fit with coarse minimizer settings is performed to find a rough estimate of the *best fit point (BFP)*. In the second stage, the fit is performed again in both octants[1] of θ_{23}, starting from the BFP of the coarse fit. For each individual fit the *MIGRAD* routine of IMINUIT [47]

is used to minimize the χ^2_{mod} fit metric defined in Equation 2.1. Iminuit is a fast, python compatible minimizer based on the MINUIT2 C++ library [48]. The individual minimizer settings for both stages are shown in Table 2.5.

To test the minimization routine and to make sure it consistently recovers any physics parameters, pseudo-data sets are produced from the MC by choosing the nominal nuisance parameters and specific physics parameters, without adding any statistical or systematic fluctuations to it. These so-called *Asimov*[2] data sets are then fit back with the full analysis chain. This type of test is called *Asimov inject/recover test*. A set of mixing values between 10^{-3} and 10^0 is injected and fit back. Without fluctuations the fit is expected to always recover the injected parameters (both physics and nuisance parameters). The fitted mixing values from the Asimov inject/recover tests are compared to the true injected values in Figure 2.3 for all three mass samples. As desired, the fit is always able to recover the injected physics parameter and the nuisance parameters within the statistical uncertainty or at an insignificant fit metric difference.

[48]: James et al. (1975), "Minuit: A System for Function Minimization and Analysis of the Parameter Errors and Correlations"

Fit	Err.	Prec.	Tol.
Coarse	1e-1	1e-8	1e-1
Fine	1e-5	1e-14	1e-5

Table 2.5: Migrad settings for the two stages in the minimization routine. *Err.* are the step size for the numerical gradient estimation, *Prec.* is the precision with which the LLH is calculated, and *Tol.* is the tolerance for the minimization.

> FInd first occurance of "Asimov" and add reference and explain it there (RED)

2: A pseudo-data set without statistical fluctuations is called Asimov data set.

Asimov Test

Figure 2.3: Asimov inject/recover test results for all three mass samples. Mixing values between 10^{-3} and 10^0 are injected and fit back with the full analysis chain. The injected parameter is always recovered within the statistical uncertainty or at an insignificant fit metric difference.

2.3.2 Goodness of Fit

To estimate the GOF, pseudo-data is generated from the MC by injecting the BFP parameters as true parameters and then fluctuating the expected bin counts to account for MC uncertainty and Poisson fluctuations in data. First, the expectation value of each bin is drawn from a Gaussian distribution centered at the nominal expectation value with a standard deviation corresponding to the MC uncertainty of the bin. Based on this sampled expectation value, each bin count is drawn from a Poisson distribution, independently, to get the final pseudo-data set. These pseudo-data sets are analyzed with the same analysis chain as the real data, resulting in a final fit metric value for each pseudo-data set. By comparing the distribution of fit metric values from this *ensemble* of pseudo-data trials to the fit metric of the fit to real data, a p-value can be calculated. The p-value is the probability of finding a value of the fit metric at least as large as the one from the data fit. Figure 2.4 shows the distribution from the ensemble tests for the 0.6 GeV mass sample and the observed value from the fit, resulting in a p-value

> Add 3D BFP-data pull distribution for one mass (they look the same, no?) (RED)

of 28.5 %. The p-values for the 0.3 GeV and 1.0 GeV are 28.3 % and 26.0 %, respectively, and the corresponding plots are shown in Section **??**. Based on this test, it is concluded that the fit result is compatible with the expectation from the ensemble of pseudo-data trials.
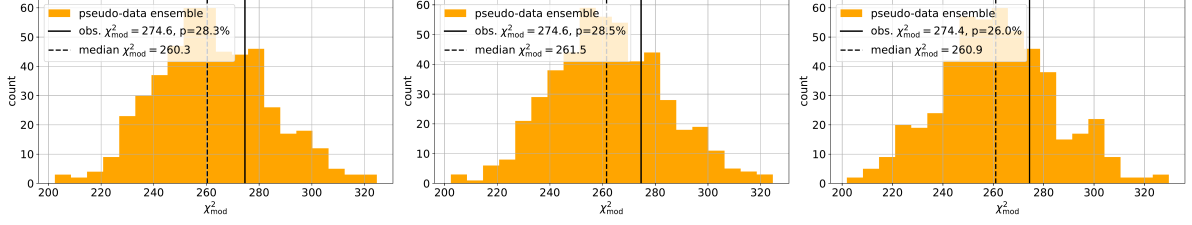

Figure 2.4: Observed fit metric and fit metric distribution from pseudo-data trials for the 0.6 GeV mass sample.

> fix dimension to fit them in one row! (RED)

2.3.3 Data/MC Agreement

> specify which they are, once I have them (RED)

At the BFP, the agreement between the data and simulation is probed by comparing the one dimensional analysis distributions for PID, energy, and cosine of the zenith angle. As an example, two distributions for the 0.6 GeV mass sample are shown in Figure **??**. The data is compared to the total MC expectation, which is also split up into the individual signal and background components for illustration. Good agreement can be observed in the pull distributions, and is quantified by a reduced χ^2, which is close to 1.0 for all distributions. The reduced χ^2 for all investigated distributions is listed in Table **??**, while the distributions themselves can be found in Section **??**.

> add 1-d data/mc agreement for example mass sample (0.6?) and all 3 analysis variables (RED)

> add table with reduced chi2 for all 1-d distributions (RED)

2.4 Results

2.4.1 Best Fit Nuisance Parameters

> Cite (again)! (RED)

> Compare here the best fit oscillation parameters to the FLERCNN results and try to quantify it, stating the pitfalls of the comparitions (satistically fully dependent) (RED)

The resulting nuisance parameter values from the fits are illustrated in Figure 2.5, where the differences to the nominal values are shown, normalized by the distance to the closest boundary. The results from all three fits are shown in the same plot and the fits prefer values of the same size for all three mass samples. For parameters that have a Gaussian prior, the $1\,\sigma$ range is also displayed. As was already confirmed during the blind fit procedure, all fitted parameters are within this range. The effective ice model parameter, N_{bfr}, prefers a value of ~ 0.74, indicating that the data fits better to an ice model that includes real birefringence effects. For completeness, the explicit results are listed in Table B.1. There, the nominal values and the absolute differences to the best fit value are also presented.

> Show best fit hole ice angular acceptance compared to nominal and flasher/in-situ fits, maybe? (YELLOW)

2.4.2 Best Fit Parameters and Limits

> Discuss what it means that the parameters are at these values? Here, or somewhere else? (RED)

The fitted mixing values are

$$|U_{\tau 4}|^2(0.3\,\text{GeV}) = 0.003^{+0.084}\,,$$
$$|U_{\tau 4}|^2(0.6\,\text{GeV}) = 0.080^{+0.134}\,,\text{and}$$
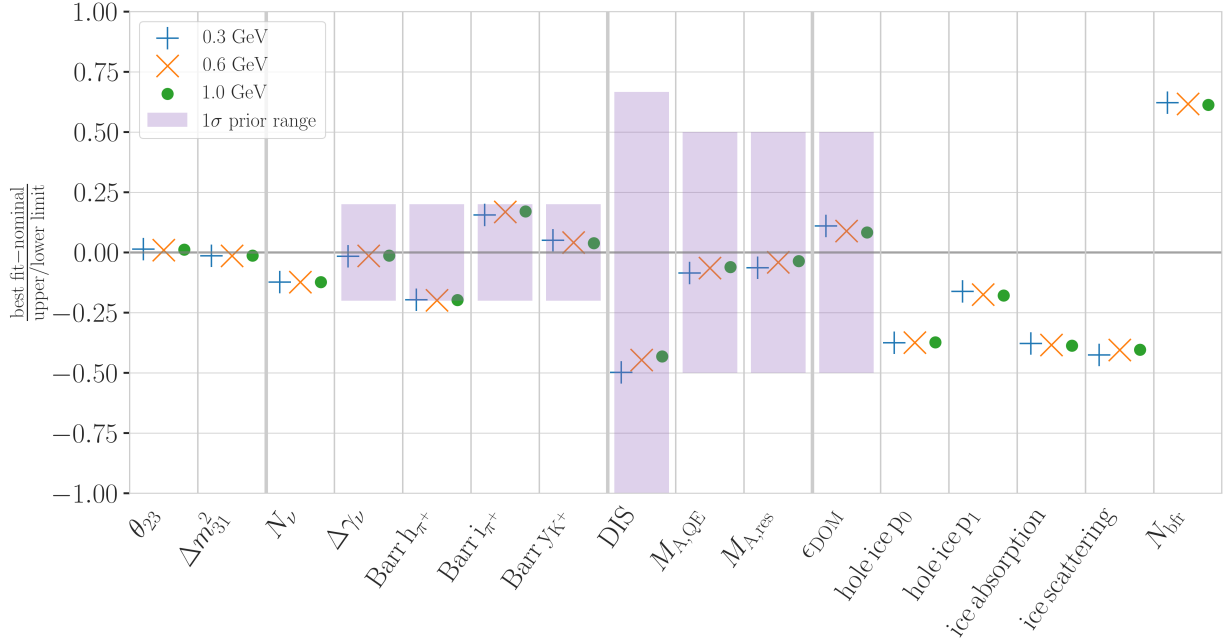$$|U_{\tau 4}|^2(1.0\,\text{GeV}) = 0.106^{+0.132}\,,$$

Figure 2.5: Best fit nuisance parameter distances to the nominal values, normalized by the distance to the closest boundary. For parameters with a Gaussian prior, the $+1\,\sigma$ range is also shown.

with their $+1\,\sigma$ uncertainty. All of them are compatible with the null hypothesis of 0.0 mixing, although the 0.6 GeV and 1.0 GeV fits indicate a mixing value of 0.08 and 0.106, respectively. The best fit mixing values and the corresponding upper limits at 68 % and 90 % *confidence level (CL)* are listed in Table 2.6, also showing the p-value to reject the null hypothesis. The CLs and p-value are estimated by assuming that *Wilks' theorem* [49] holds, meaning that the TS follows a χ^2 distribution with one degree of freedom.

[49]: Wilks (1938), "The Large-Sample Distribution of the Likelihood Ratio for Testing Composite Hypotheses"

Table 2.6: Best fit mixing values and the corresponding upper limits at 68 % and 90 % confidence level, as well as the p-value to reject the null hypothesis, estimated by assuming that Wilks' theorem holds.

HNL mass	$|U_{\tau 4}|^2$	68 % CL	90 % CL	NH p-value
0.3 GeV	0.003	0.09	0.19	0.97
0.6 GeV	0.080	0.21	0.36	0.79
1.0 GeV	0.106	0.24	0.40	0.63

Figure 2.6 shows the observed TS profiles as a function of $|U_{\tau 4}|^2$ for all three fits. The TS profile is the difference in χ^2_{mod} between the free fit and a fit where the mixing is fixed to a specific value. Also shown is the expected TS profile, based on 100 pseudo-data trials, produced at the BFP and then fluctuated using both Poisson and Gaussian fluctuations, to include the data and the MC uncertainty as was explained in Section 2.3.2. The Asimov expectation and the 68 % and 90 % bands are shown and the observed TS profiles lie within the 68 % band for all three, confirming that they are compatible with statistical fluctuations of the observed data. For the 0.3 GeV fit, the observed contour is slightly tighter than the Asimov expectation, meaning that the observed upper limits in $|U_{\tau 4}|^2$ are slightly stronger than expected. For the 0.6 GeV the opposite is the case and the observed upper limit is therefore slightly weaker than expected. For the 1.0 GeV fit, the observed upper limit is very close to the Asimov expectation in the region where the 68 % and 90 % CLs thresholds are crossed. The observed upper limits are also shown in Table 2.6.

make summary plot (masses and mixing limits on one) and then discuss wrt to other experiments? (RED)
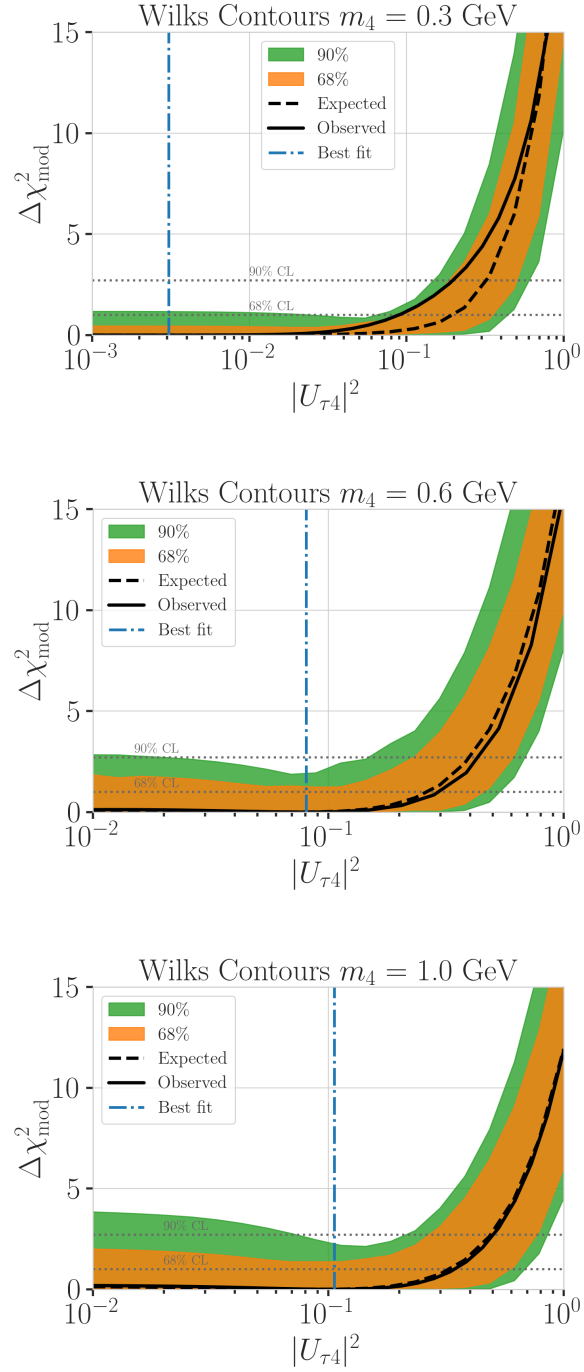
Figure 2.6: Best fit point TS profiles as a function of $|U_{\tau 4}|^2$ for the 0.3 GeV, 0.6 GeV, and 1.0 GeV mass samples. Shown are the observed profiles, the Asimov expectation at the best fit point, and the 68 % and 90 % bands, based on 100 pseudo-data trials. Also indicated are the 68 % and 90 % CL levels assuming Wilks' theorem.

APPENDIX

A

Heavy Neutral Lepton Signal Simulation

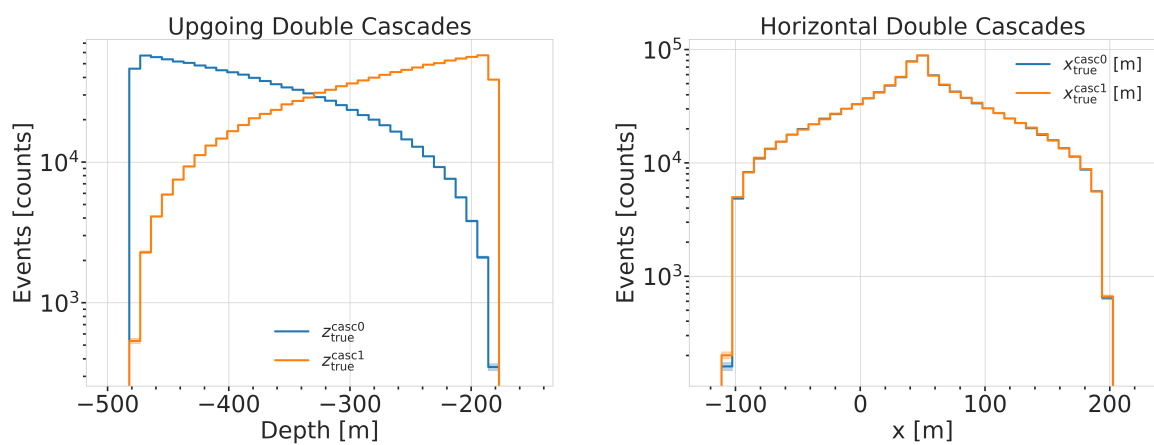## A.1 Model Independent Simulation Distributions

Figure A.1: Generation level distributions of the simplistic simulation sets. Vertical positions (left) and horizontal positions (right) of both sets are shown.

Re-make plot with x,y for horizontal set one plot!

Re-make plot with x, y, z for both cascades in one.

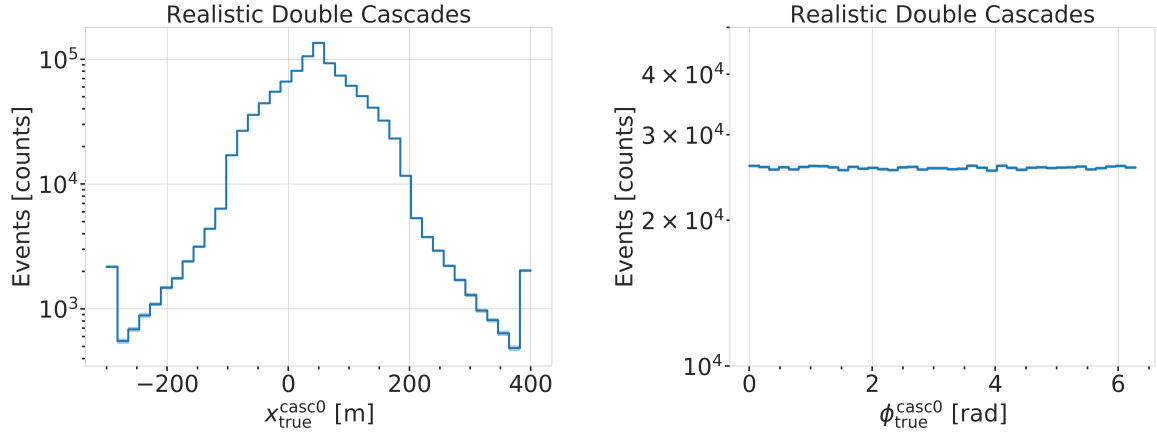Re-arrange plots in a more sensible way.

Figure A.2: Generation level distributions of the realistic simulation set. Shown are the cascade x, y, z positions (left) and direction angles (right).

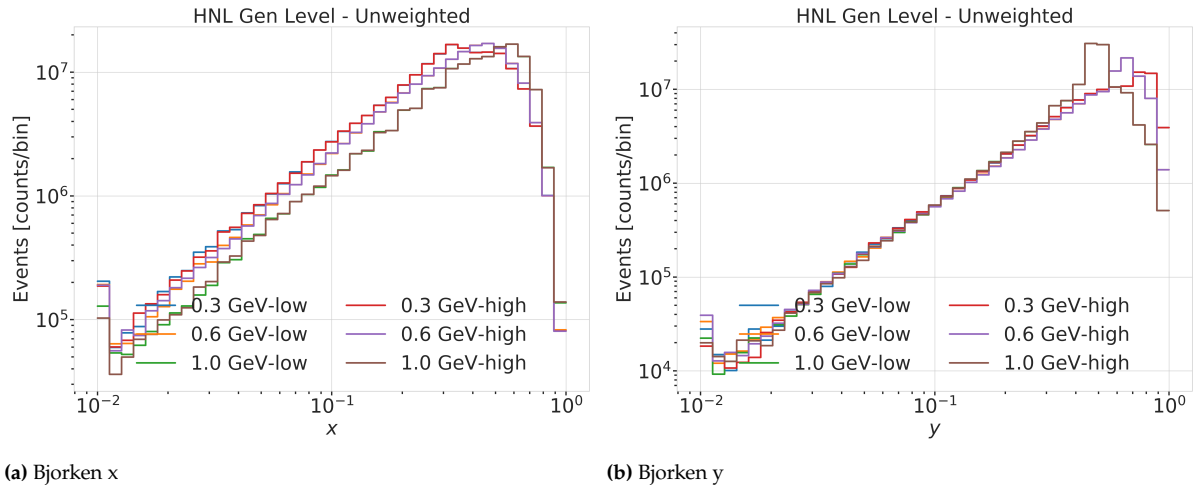## A.2 Model Dependent Simulation Distributions

(a) Bjorken x

(b) Bjorken y

Figure A.3: Generation level distributions of the model dependent simulation.

B

Analysis Results

B.1 Best Fit Nuisance Parameters

Table B.1: xx

Parameter	Nominal	Best Fit			Nominal - Best Fit		
		0.3 GeV	0.6 GeV	1.0 GeV	0.3 GeV	0.6 GeV	1.0 GeV
$\lvert U_{\tau 4}\rvert^2$	-	0.003019	0.080494	0.106141	-	-	-
$\theta_{23}[°]$	47.504700	48.117185	47.918758	48.010986	-0.612485	-0.414058	-0.506286
$\Delta m^2_{31}[\text{eV}^2]$	0.002475	0.002454	0.002454	0.002455	0.000020	0.000021	0.000019
N_ν	1.000000	0.889149	0.889055	0.889559	0.110851	0.110945	0.110441
$\Delta\gamma_\nu$	0.000000	-0.007926	-0.006692	-0.006596	0.007926	0.006692	0.006596
Barr h_{π^+}	0.000000	-0.147475	-0.148481	-0.148059	0.147475	0.148481	0.148059
Barr i_{π^+}	0.000000	0.475448	0.513393	0.521626	-0.475448	-0.513393	-0.521626
Barr y_{K^+}	0.000000	0.076176	0.062893	0.057548	-0.076176	-0.062893	-0.057548
DIS	0.000000	-0.248709	-0.223302	-0.215666	0.248709	0.223302	0.215666
$M_{\text{A,QE}}$	0.000000	-0.170528	-0.128150	-0.120345	0.170528	0.128150	0.120345
$M_{\text{A,res}}$	0.000000	-0.125855	-0.080875	-0.070716	0.125855	0.080875	0.070716
ϵ_{DOM}	1.000000	1.021984	1.017789	1.016689	-0.021984	-0.017789	-0.016689
hole ice p_0	0.101569	-0.161341	-0.161051	-0.160129	0.262910	0.262620	0.261698
hole ice p_1	-0.049344	-0.073701	-0.075596	-0.076261	0.024357	0.026252	0.026917
ice absorption	1.000000	0.943261	0.942463	0.942000	0.056739	0.057537	0.058000
ice scattering	1.050000	0.986152	0.989289	0.989438	0.063848	0.060711	0.060562
N_{bfr}	0.000000	0.746684	0.740255	0.736215	-0.746684	-0.740255	-0.736215

> fix caption and design + significant digits to show (ORANGE)

> maybe show range/prior and then deviation in sigma, or absolute for the ones without prior

Bibliography

Here are the references in citation order.

[1] C. N. Yang and R. L. Mills. "Conservation of Isotopic Spin and Isotopic Gauge Invariance". In: *Physical Review* 96.1 (Oct. 1954), pp. 191–195. DOI: 10.1103/PhysRev.96.191 (cited on page 1).

[2] S. Weinberg. "A Model of Leptons". In: *Phys. Rev. Lett.* 19 (21 Nov. 1967), pp. 1264–1266. DOI: 10.1103/PhysRevLett.19.1264 (cited on page 1).

[3] S. L. Glashow. "Partial-symmetries of weak interactions". In: *Nuclear Physics* 22.4 (Feb. 1961), pp. 579–588. DOI: 10.1016/0029-5582(61)90469-2 (cited on page 1).

[4] R. Jackiw. "Physical Formulations: Elementary Particle Theory. Relativistic Groups and Analyticity. Proceedings of the eighth Nobel Symposium, Aspenäsgården, Lerum, Sweden, May 1968. Nils Svartholm, Ed. Interscience (Wiley), New York, and Almqvist and Wiksell, Stockholm, 1969. 400 pp., illus. $31.75." In: *Science* 168.3936 (1970), pp. 1196–1197. DOI: 10.1126/science.168.3936.1196.b (cited on page 1).

[5] P. Higgs. "Broken symmetries, massless particles and gauge fields". In: *Physics Letters* 12.2 (1964), pp. 132–133. DOI: https://doi.org/10.1016/0031-9163(64)91136-9 (cited on page 1).

[6] S. Chatrchyan et al. "Observation of a New Boson at a Mass of 125 GeV with the CMS Experiment at the LHC". In: *Phys. Lett. B* 716 (2012), pp. 30–61. DOI: 10.1016/j.physletb.2012.08.021 (cited on page 1).

[7] G. Aad et al. "Observation of a new particle in the search for the Standard Model Higgs boson with the ATLAS detector at the LHC". In: *Phys. Lett. B* 716 (2012), pp. 1–29. DOI: 10.1016/j.physletb.2012.08.020 (cited on page 1).

[8] M. Gell-Mann. "A Schematic Model of Baryons and Mesons". In: *Resonance* 24 (1964), pp. 923–925 (cited on page 1).

[9] G. Zweig. "An SU(3) model for strong interaction symmetry and its breaking. Version 2". In: *DEVELOPMENTS IN THE QUARK THEORY OF HADRONS. VOL. 1. 1964 - 1978.* Ed. by D. B. Lichtenberg and S. P. Rosen. Feb. 1964, pp. 22–101 (cited on page 1).

[10] D. J. Gross and F. Wilczek. "Ultraviolet Behavior of Non-Abelian Gauge Theories". In: *PRL* 30.26 (June 1973), pp. 1343–1346. DOI: 10.1103/PhysRevLett.30.1343 (cited on page 1).

[11] C. Giunti and C. W. Kim. *Fundamentals of Neutrino Physics and Astrophysics*. Oxford University Press, Mar. 2007 (cited on page 1).

[12] M. D. Schwartz. *Quantum Field Theory and the Standard Model*. Cambridge University Press, 2013 (cited on page 1).

[13] A. Trettin. "Search for eV-scale sterile neutrinos with IceCube DeepCore". PhD thesis. Berlin, Germany: Humboldt-Universität zu Berlin, Mathematisch-Naturwissenschaftliche Fakultät, 2023. DOI: https://github.com/atrettin/PhD-Thesis (cited on pages 3, 6, 20).

[14] R. Davis, D. S. Harmer, and K. C. Hoffman. "Search for Neutrinos from the Sun". In: *Phys. Rev. Lett.* 20 (21 May 1968), pp. 1205–1209. DOI: 10.1103/PhysRevLett.20.1205 (cited on page 4).

[15] Y. Fukuda et al. "Evidence for Oscillation of Atmospheric Neutrinos". In: *Phys. Rev. Lett.* 81 (8 Aug. 1998), pp. 1562–1567. DOI: 10.1103/PhysRevLett.81.1562 (cited on page 4).

[16] Q. R. Ahmad and other. "Direct Evidence for Neutrino Flavor Transformation from Neutral-Current Interactions in the Sudbury Neutrino Observatory". In: *Phys. Rev. Lett.* 89 (1 June 2002), p. 011301. DOI: 10.1103/PhysRevLett.89.011301 (cited on page 4).

[17] S. Alam et al. "Completed SDSS-IV extended Baryon Oscillation Spectroscopic Survey: Cosmological implications from two decades of spectroscopic surveys at the Apache Point Observatory". In: *Phys. Rev. D* 103 (8 Apr. 2021), p. 083533. DOI: 10.1103/PhysRevD.103.083533 (cited on page 4).

[18] N. Aghanim et al. "Planck2018 results: VI. Cosmological parameters". In: *Astronomy & Astrophysics* 641 (Sept. 2020), A6. DOI: 10.1051/0004-6361/201833910 (cited on page 4).

[19] M. Aker et al. "Direct neutrino-mass measurement with sub-electronvolt sensitivity". In: *Nature Phys.* 18.2 (2022), pp. 160–166. DOI: 10.1038/s41567-021-01463-1 (cited on page 4).

[20] T. Asaka, S. Blanchet, and M. Shaposhnikov. "The nuMSM, dark matter and neutrino masses". In: *Phys. Lett. B* 631 (2005), pp. 151–156. DOI: 10.1016/j.physletb.2005.09.070 (cited on page 6).

[21] T. Asaka and M. Shaposhnikov. "The νMSM, dark matter and baryon asymmetry of the universe". In: *Phys. Lett. B* 620 (2005), pp. 17–26. DOI: 10.1016/j.physletb.2005.06.020 (cited on page 6).

[22] M. G. Aartsen et al. "An eV-scale sterile neutrino search using eight years of atmospheric muon neutrino1data from the IceCube Neutrino Observatory". In: *PRL* (2020) (cited on page 6).

[23] P. Astier et al. "Search for heavy neutrinos mixing with tau neutrinos". In: *Phys. Lett. B* 506 (2001), pp. 27–38. DOI: 10.1016/S0370-2693(01)00362-8 (cited on page 9).

[24] R. Acciarri et al. "New Constraints on Tau-Coupled Heavy Neutral Leptons with Masses mN=280–970 MeV". In: *Phys. Rev. Lett.* 127.12 (2021), p. 121801. DOI: 10.1103/PhysRevLett.127.121801 (cited on page 9).

[25] J. Orloff, A. N. Rozanov, and C. Santoni. "Limits on the mixing of tau neutrino to heavy neutrinos". In: *Phys. Lett. B* 550 (2002), pp. 8–15. DOI: 10.1016/S0370-2693(02)02769-7 (cited on page 9).

[26] I. Boiarska et al. "Blast from the past: constraints from the CHARM experiment on Heavy Neutral Leptons with tau mixing". In: (July 2021) (cited on page 9).

[27] P. Abreu et al. "Search for neutral heavy leptons produced in Z decays". In: *Z. Phys. C* 74 (1997). [Erratum: Z.Phys.C 75, 580 (1997)], pp. 57–71. DOI: 10.1007/s002880050370 (cited on page 9).

[28] M. Tanabashi et al. "Review of Particle Physics". In: *Phys. Rev. D* 98 (3 Aug. 2018), p. 030001. DOI: 10.1103/PhysRevD.98.030001 (cited on pages 11, 13).

[29] M. Honda et al. "Atmospheric neutrino flux calculation using the NRLMSISE-00 atmospheric model". In: *Phys. Rev. D* 92 (2 July 2015), p. 023004. DOI: 10.1103/PhysRevD.92.023004 (cited on pages 11, 21).

[30] A. Fedynitch et al. "Calculation of conventional and prompt lepton fluxes at very high energy". In: *European Physical Journal Web of Conferences*. Vol. 99. European Physical Journal Web of Conferences. Aug. 2015, p. 08001. DOI: 10.1051/epjconf/20159908001 (cited on page 11).

[31] P. A. M. Dirac. "The Quantum Theory of the Emission and Absorption of Radiation". In: *Proceedings of the Royal Society of London Series A* 114.767 (Mar. 1927), pp. 243–265. DOI: 10.1098/rspa.1927.0039 (cited on page 12).

[32] I. Esteban et al. "The fate of hints: updated global analysis of three-flavor neutrino oscillations". In: *JHEP* 09 (2020), p. 178. DOI: 10.1007/JHEP09(2020)178 (cited on page 13).

[33] A. Terliuk. "Measurement of atmospheric neutrino oscillations and search for sterile neutrino mixing with IceCube DeepCore". PhD thesis. Berlin, Germany: Humboldt-Universität zu Berlin, Mathematisch-Naturwissenschaftliche Fakultät, 2018. DOI: 10.18452/19304 (cited on page 14).

[34] J. A. Formaggio and G. P. Zeller. "From eV to EeV: Neutrino cross sections across energy scales". In: *Rev. Mod. Phys.* 84 (3 Sept. 2012), pp. 1307–1341. DOI: 10.1103/RevModPhys.84.1307 (cited on page 15).

[35] P. Coloma et al. "GeV-scale neutrinos: interactions with mesons and DUNE sensitivity". In: *Eur. Phys. J. C* 81.1 (2021), p. 78. DOI: 10.1140/epjc/s10052-021-08861-y (cited on page 15).

[36] V. Barger et al. "Matter effects on three-neutrino oscillations". In: *Phys. Rev. D* 22 (11 Dec. 1980), pp. 2718–2726. DOI: 10.1103/PhysRevD.22.2718 (cited on page 17).

[37] A. M. Dziewonski and D. L. Anderson. "Preliminary reference Earth model". In: *Physics of the Earth and Planetary Interiors* 25.4 (1981), pp. 297–356. DOI: https://doi.org/10.1016/0031-9201(81)90046-7 (cited on page 17).

[38] S. Yu and J. Micallef. "Recent neutrino oscillation result with the IceCube experiment". In: *38th International Cosmic Ray Conference*. July 2023 (cited on pages 18, 21).

[39] L. Fischer, R. Naab, and A. Trettin. "Treating detector systematics via a likelihood free inference method". In: *Journal of Instrumentation* 18.10 (2023), P10019. DOI: 10.1088/1748-0221/18/10/P10019 (cited on page 20).

[40] E. Lohfink. "Testing nonstandard neutrino interaction parameters with IceCube-DeepCore". PhD thesis. Mainz, Germany: Johannes Gutenberg-Universität Mainz, Fachbereich für Physik, Mathematik und Informatik, 2023. DOI: http://doi.org/10.25358/openscience-9288 (cited on page 20).

[41] J. Evans et al. "Uncertainties in atmospheric muon-neutrino fluxes arising from cosmic-ray primaries". In: *Phys. Rev. D* 95 (2 Jan. 2017), p. 023012. DOI: 10.1103/PhysRevD.95.023012 (cited on page 21).

[42] J. Feintzeig. "Searches for Point-like Sources of Astrophysical Neutrinos with the IceCube Neutrino Observatory". PhD thesis. University of Wisconsin, Madison, Jan. 2014 (cited on page 21).

[43] N. Kulacz. "In Situ Measurement of the IceCube DOM Efficiency Factor Using Atmospheric Minimum Ionizing Muons". MA thesis. University of Alberta, 2019 (cited on page 21).

[44] M. G. Aartsen et al. "Computational techniques for the analysis of small signals in high-statistics neutrino oscillation experiments". In: *Nucl. Instrum. Meth. A* 977 (2020), p. 164332. DOI: 10.1016/j.nima.2020.164332 (cited on page 22).

[45] https://github.com/icecube/pisa (cited on page 22).

[46] R. S. Nickerson. "Confirmation Bias: A Ubiquitous Phenomenon in Many Guises". In: *Review of General Psychology* 2 (1998), pp. 175–220 (cited on page 22).

[47] H. Dembinski et al. *scikit-hep/iminuit: v2.17.0*. Version v2.17.0. Sept. 2022. DOI: 10.5281/zenodo.7115916 (cited on page 22).

[48] F. James and M. Roos. "Minuit: A System for Function Minimization and Analysis of the Parameter Errors and Correlations". In: *Comput. Phys. Commun.* 10 (1975), pp. 343–367. DOI: 10.1016/0010-4655(75)90039-9 (cited on page 23).

[49] S. S. Wilks. "The Large-Sample Distribution of the Likelihood Ratio for Testing Composite Hypotheses". In: *The Annals of Mathematical Statistics* 9.1 (1938), pp. 60–62. DOI: 10.1214/aoms/1177732360 (cited on page 25).